



Brain Activity in Threat Situations

Carolina Almeida Lopes

Thesis submitted to the Faculty of Sciences and Technology of the University of Coimbra for the degree of Master in Biomedical Engineering with specialization in Clinical Informatics and Bioinformatics.

Supervisors:

Prof. Dr. Lorena Itatí Petrella (DEI)

Prof. Dr. César Alexandre Domingues Teixeira (DEI)

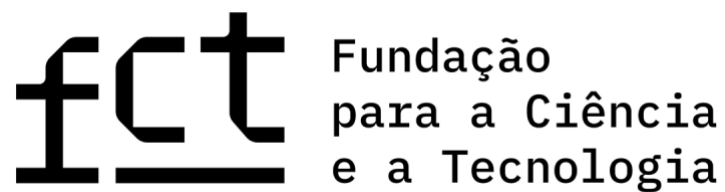
Coimbra, 2023

This work was developed at

Center for Informatics and Systems of the University of Coimbra



This work is funded by FCT- Foundation for Science and Technology, I.P., within the scope of the projects: CISUC - UID/CEC/00326/2020 with funds from the European Social Fund, through the Regional Operational Program Centro 2020; and project RECoD - PTDC/EEI-EEE/5788/2020 financed with national funds (PIDDAC) via the Portuguese State Budget.



Acknowledgments

The completion of this project marks the end of an important journey. An enriching, challenging, difficult, full of ups and downs journey but, above all, a beautiful one. It was 5 years of a lot of work, effort and commitment, but also full of wonderful memories. Therefore, I could not fail to thank everyone who was present and who accompanied me throughout this journey and without whom it would not have the same meaning.

Firstly, I would like to thank my supervisors Professor Lorena Petrella and Professor César Teixeira for all their support, for all the transmitted knowledge and for all the hours of discussion, suggestions and clarifications given throughout the course of this project. It was, without a doubt, an essential and huge help that allowed the realization of this project.

To Doctor Jaime, for all the help and guidance provided during the EEG acquisitions and for his availability and time spent, which contributed to the acquisitions being as successful as possible.

To my parents, who always supported me and never let me lack anything. Thank you for investing in my future and for making these 5 years possible. What I achieved was thanks to your efforts, your support, your teachings and the trust you always placed in me.

To all my friends, both those who were already part of my life before and those that Coimbra gave me. Thank you for all the moments, for the laughter, for the joys, for the sadness, for the study evenings, for the nights. Without your support, this journey would not have been as important as it was.

A special thank you to Ana Gabriela, Ana Marques, Catarina, Inês and Angélica who were always by my side, day after day, throughout these 5 years that, despite being long, went by too quickly. My journey would not have been the same without all the moments shared year after year, and I know that this is just the beginning of a long lasting beautiful friendship.

Finally, thank you to Coimbra, the city that became home, where I grew up and created a family for life.

Abstract

It has been proved that threat stimuli evoke a defensive response and trigger physiological reflexes. The study of brain activity under the appearance of an unexpected threat situation detected by the visual system can give some insights into how the brain reacts to potential dangers and threats, and how the defensive response is originated.

Past studies have used electroencephalography (EEG) and functional magnetic resonance imaging (fMRI) to identify the brain areas activated in response to a threatening stimulus. While fMRI provides good spatial resolution, EEG warrants better temporal resolution. Regarding the threatening stimulus used in previous studies, most of them resorted mainly to images, videos, and sounds, which induced emotional responses related to a threatening situation. Although, these studies did not provide an immersive scene, reducing the feeling of being under threat.

In this project, a virtual reality (VR) video is used to present an unexpected threat in a calm scene with the aim of invoking a defensive reaction. The threat consisted of a neutral object approaching quickly towards the observer and was designed with the aim of reducing induced emotions related to the stimulus itself. While the video is observed, brain activity is measured using EEG, providing good temporal resolution. The main goal of this project is to study the brain areas involved in the threatening situation, and the functional connectivity between those areas in order to depict the flow of information.

The results show that the inferior frontal gyrus, premotor cortex, supplementary motor cortex, prefrontal cortex, superior temporal gyrus, middle temporal gyrus, associative visual cortex, primary motor cortex and primary somatosensory cortex are involved in the processing of threatening situations. Also, the relevance of delta, beta and gamma frequency bands in threat processing was evidenced. Regarding the connectivity analysis, the relevant functional connections are concentrated in the front half of the brain. There is a flux of information from the left inferior frontal gyrus and left middle temporal gyrus to the motor areas (primary motor

cortex and premotor cortex), as well as a flux of information from the premotor cortex to the primary motor cortex. The remaining relevant connections involve the prefrontal cortex.

The results obtained in this study provide new insights about the brain functioning under threat stimuli, and may subsequently contribute to the delineation of therapeutic approaches in some psychiatric conditions.

Keywords: brain, threat, defensive reaction, vision, electroencephalogram, virtual reality

Resumo

Já foi provado que um estímulo ameaçador evoca uma resposta defensiva e desencadeia reflexos fisiológicos. O estudo da ativação cerebral resultante de uma ameaça visual inesperada pode fornecer informação sobre como o cérebro reage a potenciais perigos e ameaças, e como são originadas as respostas defensivas.

Estudos anteriores usaram eletroencefalografia (EEG) e ressonância magnética funcional (fMRI) para identificar as áreas cerebrais ativadas em resposta a um estímulo ameaçador. Embora o fMRI forneça boa resolução espacial, o EEG garante melhor resolução temporal. Quanto aos estímulos utilizados em estudos anteriores, a maioria recorre principalmente a imagens, vídeos e sons que induzem respostas emocionais relacionadas a uma situação ameaçadora. Porém, esses estudos não proporcionaram uma cena imersiva, reduzindo a sensação de estar sob ameaça.

Neste projeto, é utilizado um vídeo de realidade virtual (RV) para apresentar uma ameaça inesperada numa cena calma, com o objetivo de invocar uma reação defensiva. A ameaça consiste num objeto neutro aproximando-se rapidamente do observador e foi pensada com o objetivo de reduzir emoções induzidas pelo próprio estímulo. Enquanto o vídeo é visualizado, a atividade cerebral é medida com EEG, proporcionando boa resolução temporal. O principal objetivo deste projeto é estudar as áreas cerebrais envolvidas na situação de ameaça e a conectividade funcional entre essas áreas com o propósito de obter o fluxo de informação.

Os resultados mostram que o giro frontal inferior, o córtex pré-motor, o córtex motor suplementar, o córtex pré-frontal, o giro temporal superior, o giro temporal médio, o córtex visual associativo, o córtex motor primário e o córtex somatossensorial primário estão envolvidos no processamento de situações de ameaça. É também evidenciada a relevância das bandas delta, beta e gama no processamento de situações de ameaça. Em relação à análise de conectividade, as conexões cerebrais relevantes estão concentradas na metade frontal do cérebro. Há um fluxo de informação do giro frontal inferior esquerdo e do giro temporal médio

esquerdo para as áreas motoras (córtex motor primário e córtex pré-motor), assim como do córtex pré-motor para o córtex motor primário. As restantes conexões relevantes encontradas envolvem o córtex pré-frontal.

Os resultados obtidos neste estudo fornecem novos insights sobre o funcionamento do cérebro durante uma situação de ameaça, podendo posteriormente contribuir para o delineamento de abordagens terapêuticas para algumas condições psiquiátricas.

Palavras-chave: cérebro, ameaça, reação defensiva, visão, eletroencefalograma, realidade virtual

Contents

Acknowledgments	5
Abstract	6
Resumo	8
Contents	10
List of Figures	13
List of Tables.....	15
List of Equations.....	16
List of Abbreviations	17
1. Introduction	19
1.1. Context and Motivation.....	19
1.2. Objective.....	20
1.3. Thesis Outline	20
2. Background Concepts.....	22
2.1. The Brain.....	22
2.2. The Central Visual System	23
2.3. Threat and Unexpected Visual Stimuli.....	24
2.4. Fear and Brain.....	25
2.5. Defensive Response.....	27
2.6. Human Visual Reaction Time	28
2.7. Visual Evoked Potential.....	28
2.8. Electroencephalography	29
2.9. Brain Waves.....	30
2.10. EEG Electrode Placement.....	31
2.11. EEG Artifacts	32
2.11.1. Eye Blink and Movements.....	33
2.11.2. Non-ocular Muscular Activity	34

2.11.3. Cardiac Artifact	34
2.11.4. Extrinsic Artifacts	35
2.12. Signal Processing	35
2.12.1. Independent Component Analysis	35
2.12.2. Filters.....	36
2.12.3. Short-Time Fourier Transform	37
2.12.4. Wavelet Transform	37
2.13. Feature Extraction.....	37
2.13.1. Time Domain Features	38
2.13.2. Frequency Domain Features.....	38
2.13.3. Entropy	39
2.14. Functional Connectivity	39
2.15. Virtual Reality.....	40
2.15.1. Definition	40
2.15.2. VR Applications.....	41
3. State-of-the-Art	42
3.1. Related EEG Datasets.....	42
3.2. Overview of Related Works	42
4. Materials and Methods.....	47
4.1. Experiment Development.....	47
4.1.1. Virtual Reality Equipment	47
4.1.2. Visual Stimulus	48
4.1.3. EEG Acquisition System and Electrode Placement	51
4.1.4. Stimulus and EEG Recording Synchronization	52
4.1.5. Participants and Ethical Aspects.....	52
4.1.6. Procedure	53
4.2. Signal Processing.....	54
4.2.1. Remove Excess Data	55
4.2.2. Filtering.....	55
4.2.3. Artifacts Removal	56
4.2.4. Feature Extraction.....	56
4.3. Identification of Relevant Brain Areas	57
4.3.1. Data Distribution Test	57
4.3.2. Statistical Significance Test	57

4.4. Functional Connectivity Between Relevant Brain Areas	60
4.4.1. Coherence and Imaginary Part of Coherence	63
4.4.2. Weighted Phase Lag Index.....	65
4.4.3. Mean Phase Coherence.....	65
4.4.4. Directed Transfer Function	66
4.5. Frequency Bands Connectivity Analysis	67
5. Results and Discussion.....	68
5.1. Preliminary Visual Analysis of Extracted Features	68
5.2. Relevant Brain Areas	70
5.2.1. Results	70
5.2.2. Relevant Threat Brain Areas and Frequency Bands Discussion	71
5.2.2. Overall Discussion	75
5.3. Functional Connectivity Between Relevant Brain Areas	77
5.3.1. COH, iCOH, wPLI and MPC Results.....	77
5.3.2. Discussion	84
5.4. Threat Brain Network	85
5.4.1. Results	85
5.4.2. Discussion	86
5.5. Frequency Bands Connectivity Analysis	87
5.5.1. Results	88
5.5.2. Discussion	88
6. Acquired Competencies	90
7. Conclusion	92
References.....	94
Annex 1.....	100
Annex 2.....	105

List of Figures

Figure 1. The different regions of the brain (Extracted from [10])	18
Figure 2. Schematic representation of the human visual system (Extracted from [12])	18
Figure 3. Core network of fear processing in healthy individuals (Extracted from [17])	20
Figure 4. Wave representation of the five EEG rhythms (Extracted from [37])	22
Figure 5. Schematic representation of the EEG 10–20 system (Extracted from [38])	26
Figure 6. Example of artifacts introduced by eye blinks in EEG data (Extracted from [42]) ..	27
Figure 7. Example of artifacts introduced by eye movements in EEG data (Extracted from [41])	29
Figure 8. Example of artifacts introduced by muscle activity in EEG data (Extracted from [42])	29
Figure 9. Example of a VR system (Extracted from [70])	30
Figure 10. Cortical networks activated by looming visual stimuli in marmoset monkeys (Extracted from [7])	35
Figure 11. Scheme of the general experimental setup steps	47
Figure 12. HP Reverb G headset (Extracted from [80])	39
Figure 13. Example of four frames of the developed VR video; a) presents a neutral part of the video; b) and c) present the moment of the rock appearance ; d) shows the moment of the bird appearance	42
Figure 14. Video timeline with the instants of the three presented stimuli	44
Figure 15. NeuroEvolution EEG Electro-Cap International (Extracted from [84])	44

Figure 16. Example of a participant along the experimental procedure, with the EEG cap and VR headset connected	45
Figure 17. Scheme of the signal processing steps	47
Figure 18. Example of the Kruskal-Wallis test for the F8 delta band and for the threat stimulus case	52
Figure 19. Example of a spectrogram for channel T4, where T, S and B represent the instants of the threat, sound and bird stimuli, respectively	60
Figure 20. Example of the boxplots for the beta band of channel T4, for the threat stimulus. Each boxplot represents one of the four time instants: $t(\text{neutral})$, and $t(\text{stimulus})$, $t(\text{stimulus}+1)$ and $t(\text{stimulus}+2)$ which represent the three consecutive instants immediately after the threat stimulus appearance, as described in section 4.3.2	61
Figure 21. Relevant channels and frequency bands in the threat stimulus situation. Relevant channels are marked in blue	68
Figure 22. Pre stimulus, pos stimulus and pos-pre stimulus COH matrices and pos-pre stimulus brain connectivity representation	72
Figure 23. Pre stimulus, pos stimulus and pos-pre stimulus iCOH matrices and pos-pre stimulus brain connectivity representation	72
Figure 24. Pre stimulus, pos stimulus and pos-pre stimulus wPLI matrices and pos-pre stimulus brain connectivity representation	73
Figure 25. Pre stimulus, pos stimulus and pos-pre stimulus MPC matrices and pos-pre stimulus brain connectivity representation	74
Figure 26. Schematic representation of the brain connectivity and directionality (represented by arrows) found for the threat situation.....	80
Figure 27. COH matrices for all the frequency bands	83

List of Tables

Table 1. Characteristics of the five EEG rhythms [11], [35], [36]	26
Table 2. Characteristics of each EEG files	48
Table 3. Post-stimuli time-windows analyzed for each of the stimuli	51
Table 4. EEG channels and frequency bands that presented significant differences between the neutral state and each of the 3 stimuli, using a significance level of 0.05	62
Table 5 Channel connections that presented significant differences between the neutral state and the threat stimulus state for each of the connectivity methods, using a significance level of 0.05, and after the multiple comparison correction	75
Table 6: Channel connections that presented significant differences between the neutral state and the threat stimulus state for each of the connectivity methods, using a significance level of 0.01, without multiple comparison correction	75
Table 7: Channel connections presenting differences between the connectivity values of the threat stimulus and neutral states (pos-pre) higher than the 0.65-quantile for each of the connectivity methods, and connections in common with at least three of the methods (in the last column). The values in bold represent the connections with the highest Pos-Pre connectivity values of each method	76

List of Equations

Equation 1. Cross spectral density	56
Equation 2. Normalized cross-spectrum	56
Equation 3. Coherence	56
Equation 4. Imaginary part of coherence	56
Equation 5. Weighted phase lag index	57
Equation 6. Instantaneous phase of a signal	58
Equation 7. Mean phase coherence	58
Equation 8. Directed transfer function	58

List of Abbreviations

ANS Autonomic Nervous System

AR Autoregressive

COH Coherence

CNS Central Nervous System

CWT Continuous Wavelet Transforms

DE Differential Entropy

DTF Directed Transfer Function

DWT Discrete Wavelet Transform

ECG Electrocardiogram

EEG Electroencephalogram

ERO Event Related Oscillations

ERP Event Related Potential

FDR False Discovery Rate

FIR Finite Impulse Response

fMRI Functional Magnetic Resonance Imaging

fps Frames per Second

Hz Hertz

ICA Independent Component Analysis

iCOH Imaginary Part of Coherency

iEEG intracranial Electroencephalography

IIR Infinite Impulse Response

MI Mutual Information

MPC Mean Phase Coherence

MRI Magnetic Resonance Imaging

MVAR Multivariate Autoregressive Model

MVPA Multi-Voxel Pattern Analysis

PET Positron Emission Tomography

PLI Phase Lag Index

PLV Phase-Locking Value

PNS Peripheral Nervous System

PPS Peripersonal Space

PSD Power Spectral Density

PSI Phase Slope Index

PTSD Post-Traumatic Stress Disorder

SNR Signal-to-Noise-Ratio

SNS Somatic Nervous System

STFT Short Time Fourier Transform

VEP Visual Evoked Potential

VR Virtual Reality

wPLI weighted Phase Lag Index

ZCR Zero-Crossing Rate

1. Introduction

1.1. Context and Motivation

The study of brain activity under the appearance of an unexpected threat detected by the visual system can give some insights into how the brain reacts to potential dangers and threats, and how the defensive response is originated. This can consequently impact the diagnosis and treatment of diverse neurological conditions, involving neurostimulation.

It has been proved that threat stimuli evoke a defensive response and trigger physiological reflexes affecting ongoing behavior. In humans, some studies found diverse brain regions that activate under threatening stimuli namely cortical areas such as the premotor cortex, the pre-supplementary motor area and the inferior frontal gyrus [1]–[3].

There are studies conducted with humans, monkeys, and even other species. To identify the activated brain areas, some of them use electroencephalogram (EEG) [4]–[6], while others use functional magnetic resonance imaging (fMRI) [1]–[3], [7]. However, despite a good spatial resolution, fMRI has a poor temporal resolution, which limits the study of fast responses [8].

Regarding the threatening stimulus applied, most of the studies resort mainly to images, videos played on a monitor, and sounds. Some applied stimuli involve frightening animals, human reactions to a threat situation (such as face or body expressions) [1], [6], looming visual stimuli [2], [4], [7], exposure to heights [5] or other situations [3]. However, in all these cases, emotional responses are inherent to visual stimuli recognition and interpretation. Moreover, observing a scene on a monitor reduces the person's feeling of being in a threatening situation.

1.2. Objective

In this study, a virtual reality (VR) video is used to present an unexpected visual threat in a calm scene to invoke a defensive reaction, while brain activity is being measured using EEG. Using EEG ensures a good temporal resolution (in order of milliseconds).

The main goal of the project is to study the brain activation pattern during a threatening situation, that is, to find the specific brain areas activated after the appearance of a threatening stimulus. More specifically, it is intended to generate an escape response with the stimulus produced by VR (more than an emotional response which happens with most of the stimuli used in the studies carried out to date), identify the changes in EEG patterns in different brain regions and analyze the functional connectivity between brain regions in threat situations.

Therefore, this project is expected to improve the knowledge about reflex reactions under threat situations and the cortical connections involved in the process.

1.3. Thesis Outline

This document describes all the steps of the work developed during the project, from the background concepts and the state-of-the-art review to the results and conclusions of the project itself. The document is organized into seven chapters, whose contents are summarized below.

- 1. Introduction:** Describes the problem, context and motivation behind this study and its main objectives.
- 2. Background Concepts:** Presents and explains key background concepts necessary for the study development.
- 3. State-of-the-Art:** Presents a review of the literature and a list of studies carried out to date with a summary of the main methodological aspects, results and conclusions reached in each of them.
- 4. Materials and Methods:** Describes all the methods employed throughout the experimental work, including the VR video development and preparation, the brain activity acquisition through EEG, signal processing, feature extraction and statistical analysis.
- 5. Results and Discussion:** Reports the results obtained in the study as well as their analysis and discussion.

6. Acquired Competencies: Describes the skills acquired during the development of the project.

7. Conclusion: Presents the main conclusions of this study

2. Background Concepts

2.1. The Brain

The nervous system is subdivided into the central nervous system (CNS) composed of the brain and spinal cord, and the peripheral nervous system (PNS) which comprises the somatic nervous system (SNS) and the autonomic nervous system (ANS) [9].

The brain is the principal organ of the nervous system, responsible for controlling, integrating, processing, and coordinating the information it receives. It also controls movement, communication, language, senses, emotions, memory and thinking [9].

The human brain is divided into the cerebrum, cerebellum, and brainstem (Figure 1).

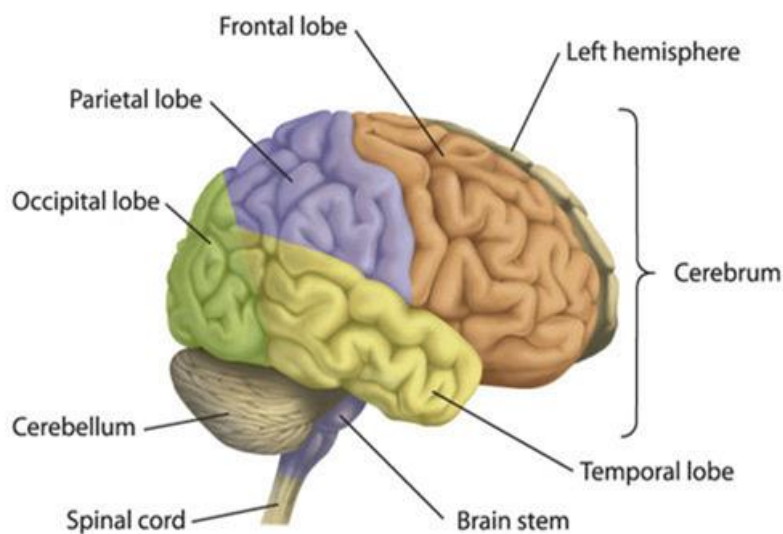


Figure 1: The different regions of the brain (Extracted from [10]).

The cerebrum's main functions are related to the control of sensory and motor information, and conscious and unconscious behaviors, feelings, and memory. The outer layer is the cerebral cortex. It's also divided into the right and left cerebral hemispheres, which in turn are composed of the frontal, parietal, temporal and occipital lobes. The cerebellum contains the

cerebellar cortex and deep cerebellar nuclei and is connected to the brainstem by the cerebellar peduncles. Its main function is to control the coordination of voluntary movement and balance. Finally, the brainstem lies between the base of the cerebrum and the spinal cord and is divided into the medulla, pons, and midbrain. It connects the cerebrum and cerebellum to the spinal cord [9].

2.2. The Central Visual System

The visual sensory information is extracted by the retina and analyzed by the central visual system (Figure 2). Visual perception is carried out by the lateral geniculate nucleus of the thalamus and by the primary visual cortex, also called the striate cortex. Visual perception refers to the ability to receive, interpret and react to visual stimuli. The information is processed in parallel by neurons specialized for the analysis of different stimulus attributes and then goes to different extrastriate cortical areas in the temporal and parietal lobes [11].

The pathway that starts at the optic nerve and leaves the retina towards the brain stem is called **retinofugal projection**. This projection englobes the optic nerve, the optic chiasm, and the optic tract (Figure 2). The retinal ganglion cells project axons into the lateral geniculate nucleus, the hypothalamus, and the midbrain. Neurons from the lateral geniculate nucleus then project axons to the primary visual cortex. However, the lateral geniculate nucleus also receives inputs from the brain stem related to attentiveness and alertness [11].

There are two main cortical streams of visual processing beginning in the striate cortex that project in different ways: **the ventral stream that projects ventrally towards the temporal lobe and the dorsal stream that projects dorsally towards the parietal lobe**. The ventral stream oversees recognition of objects and visual perception. The dorsal stream is involved in the visual control of action and the analysis of visual motion [11].

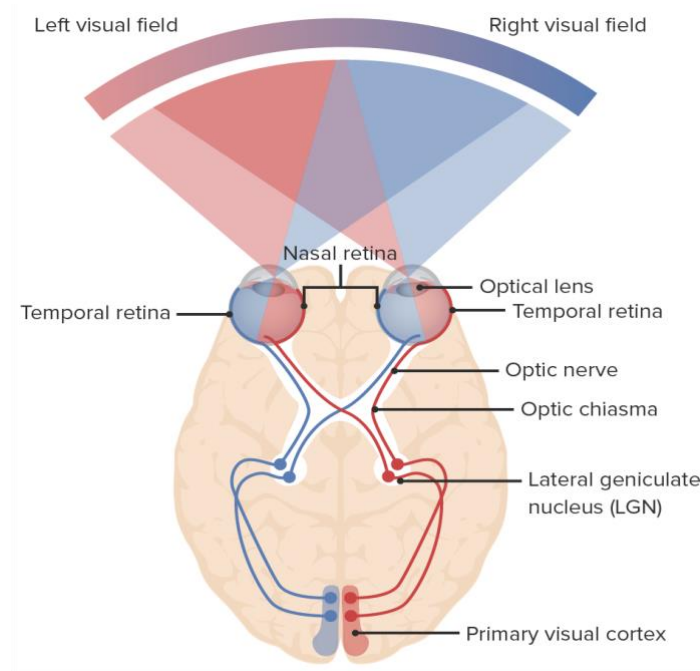


Figure 2: Schematic representation of the human visual system (Extracted from [12]).

2.3. Threat and Unexpected Visual Stimuli

The visual system plays an important role in protecting the body from threats once it's the primary sense used by humans to evaluate and respond to threats. A threat is an impending source of danger that has the potential to cause harm or damage. There are several types and forms of threats that can range from a frightening animal to something that suddenly appears in the field of vision.

An example of an unexpected visual threatening stimulus is a looming visual stimulus like an unexpected approaching object that, when perceived as a threat, triggers a rapid defensive or evasive behavior, according to its survival value. Being able to perceive motion such as looming stimuli is needed to adapt the behavior to the situation [4], [5], [7], [13].

The concept of visual looming is consequently related to the concept of peripersonal space (PPS) which concerns the space surrounding the body. Specific sets of neurons encode the

location of stimuli approaching the body to generate consequent motor responses such as actions towards approaching objects or defensive reactions as a response to the threat located in the PPS. In the case of a looming stimulus, the consequent optical expansion on the retina indicates the time to collision of that object. Studies have shown that perceived time to collision depends on the content of the stimuli, with threatening stimuli having a lower perceived time to collision than non-threatening stimuli, indicating that threatening stimuli are detected faster. Also, past research shows that collision judgments result in the activation of the left inferior parietal cortex, left ventral premotor cortex, and left sensorimotor cortex implying the role of these brain areas in temporal prediction. This sensorimotor response implies the existence of a motor preparation resulting from a looming stimulus even when execution is not intended [4], [5], [7], [13]–[16].

Additionally, past research has shown that the direction of the threat, that is, if it's coming towards or away from the person, can alter brain activity and psychological responses [3].

2.4. Fear and Brain

A threatening stimulus as well as the natural defensive reaction that can result from it, are largely associated with emotions, especially with fear. Fear can be characterized as a physiological state, and an emotion caused by the threat of danger, pain, or harm, that evokes defensive responses involving autonomic and hormonal changes. This emotion can result from visual stimuli that can be interpreted as a threat such as looming predators, environmental disasters, dangerous situations, or social threats [17], [18].

Fear processing can be divided into two distinct conditions: explicit and implicit fear processing. Regarding explicit fear processing, in the presence of conscious awareness, the fearful content of the stimulus is intuitive and rapidly recognized. On the other hand, implicit fear processing implies unawareness of the presence and content of the stimulus [17].

Diverse brain areas and structures are specifically correlated with the recognition, expression and processing of emotions involving a wide range of the nervous system.

Therefore, the human reaction to emotions is a consequence of a lot of factors such as sensory stimuli, brain circuitry and neurotransmitters [1], [11], [19].

Regarding the brain areas involved in implicit and explicit fear processing, a common neural network was identified (Figure 3). This core neural network involves subcortical regions such as the amygdala and pulvinar areas, as well as fronto-occipital regions such as inferior occipital gyrus, inferior frontal gyrus, and fusiform gyrus [17].

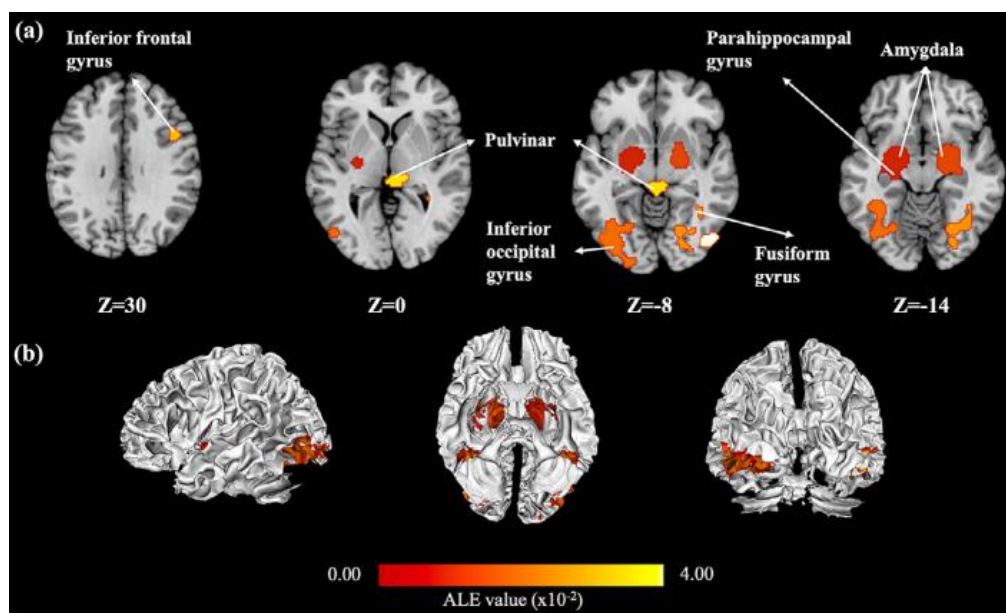


Figure 3: Core network of fear processing in healthy individuals (Extracted from [17]).

The amygdala is one of the most relevant structures involved in emotional reaction and is crucial for fear processing, regardless of the applied stimulus and awareness level. It's a complex of nuclei divided into the corticomedial nuclei, basolateral nuclei and central nucleus, and is in the medial temporal lobe. All sensory systems are connected to the amygdala which allows the integration of the information carried by them. For instance, the basolateral nuclei receive tactile, visual, auditory, and gustatory afferents while the corticomedial nuclei receive olfactory afferents. The amygdala is connected to regions of the cortex like the medial, orbital and lateral prefrontal cortex. Studies have shown that most of the injuries involving the

amygdala result in the inability to recognize fear in facial expressions. It has also been found that the amygdala is very sensitive to threatening stimuli and increases vigilance [1], [11], [19].

The other subcortical region involved in fear processing, the pulvinar, is linked to the visual cortex and fronto-parietal attention network and has been found to be important in visual attention. Moreover, the cortical connections with the ventrolateral pulvinar are crucial to keep the cortex in an active state [17].

Regarding the fronto-occipital regions, the visual regions identified as being involved in fear (fusiform gyrus and inferior occipital gyrus) are crucial occipital regions activated as a result of negative emotional visual stimuli [17].

Considering particularly the explicit fear processing case, more activated regions have been found at the parahippocampal gyrus and pulvinar, indicating the importance of visual attention, visual orientation, and contextual association in this case. Regarding implicit fear processing, the cerebellum-amygdala-cortical pathway is the one that stands out and plays a major role [17].

2.5. Defensive Response

Defensive responses consist of the reactions to potential dangers or threats, and include avoidance responses, flight, freezing and risk assessment. An avoidance behavior, for instance, consists of efficient and fast actions directed to avoid or minimize the negative consequences of the perceived unpleasant situation. The type of defensive response depends on the threat faced and on the situation in which it is encountered, as well as its distance, proximity, and imminence. It is a survival mechanism which helps to protect and prepare the body from potential danger, and has evolved to adapt to a variety of aversive states [20], [21].

Defensive reactions were found to be linked to a brain circuit from the ventromedial prefrontal cortex, the hippocampus and the amygdala to the periaqueductal gray [1], [22].

2.6. Human Visual Reaction Time

The elapsed time for a human being able to perceive visual stimuli has been studied recurring to the reaction time. Reaction time is defined as the time interval occurring from the presentation of visual stimuli to the associated subject's immediate motor response, reflecting the conclusion of a perception process. This time encompasses the consecutive activities of the various visual areas involved, which is, approximately, 150 ms to 200 ms [23].

On the other hand, in 2013, Potter *et al.* did an experiment to find out how long a stimulus needs to be presented to be detected by the observer. In the experiment, participants were asked to look for a particular image in a sequence of different images. The image exposure time was gradually decreased, using values of 80 ms, 53 ms, 40 ms, 27 ms and 13 ms. The results of this study showed that the human brain can process images with an exposure time as low as 13 ms. In this way, the meaning of an image can be extracted even when it is in a sequence presented at 13 ms per image, which corresponds to a frame rate of about 75 fps (frames per second) [24], [25].

2.7. Visual Evoked Potential

The visual evoked potential (VEP) is involved in the visual processing and depends on the stimulus content [4].

It's a non-invasive method for visual response analysis, using electrodes placed in the occipital region of the scalp for recording brain activity while a visual stimulus is presented. It's a complex response consisting of multiple components rather than a single signal. More specifically, VEP expresses the neuronal electrical activity of the visual pathways responding to stimuli and it does not depend on the individual's state of consciousness and attention. VEP provides information about the state of the visual system and the integrity of the various structures of the visual pathway, such as slow neuronal transmission. Depending on the type

and specificities of the applied stimulus, VEPs can transmit different information [26], [27, p. 34], [28].

2.8. Electroencephalography

Electroencephalography, or EEG, is, in a most traditional setup, a minimally invasive method used to record brain rhythms and to analyze the generalized activity of the cerebral cortex, that is, it records the brain's electrical activity providing functional brain information. However, EEG collected at the scalp level can only measure the cumulative activity of large populations of cortical neurons. On the other hand, subcortical structures, such as the amygdala, don't generate large summated dipoles because its neurons' electric fields are usually oriented in different directions, meaning that neuron's activity tends to cancel among each other. This consequently precludes their activity to be registered by scalp level EEG [9], [11], [29]. Scalp EEG consists of a set of electrodes fixed to specific positions on the head. In turn, these electrodes are linked to amplifiers and recording devices. The voltages measured by the EEG are generated by the currents that flow during synaptic excitation [11].

Although it has a poorer spatial resolution when compared to other methods like positron emission tomography (PET) or magnetic resonance imaging (MRI), which have a typical spatial resolution of a few millimeters, EEG is a technology with a much higher temporal resolution allowing to measure and give detailed information about fast voltage fluctuations. Thus, while PET and MRI have temporal resolutions of some seconds, EEG registered with conventional equipment has resolutions in the order of milliseconds. This way, being a non-invasive, easy to use and low cost technique compared to others, EEG allows the study of certain neurological diseases and other biological conditions, being one of the most useful and relevant resources nowadays for the evaluation of brain activity [11], [30], [31].

2.9. Brain Waves

Brain waves are defined as oscillating electrical voltages that occur in the brain and are measured using an EEG. An EEG signal measured between electrodes on the scalp is composed of a set of waves each with specific characteristics. Also, every person has unique brain wave patterns [32].

The five EEG rhythms are delta, theta, alpha, beta, and gamma and are associated to different states of behavior, pathology, consciousness, and cognitive processes and to different frequencies as presented in Table 1. Also, an example of their waveform is present in Figure 4 [11], [33], [34].

However, different brainwave frequencies are not unique to a specific state. Although certain frequencies are more associated with certain brain states, they can also be present in other situations less commonly associated with them.

Table 1: Characteristics of the five EEG rhythms [11], [35], [36].

Brain Wave	Frequency Range	Brain States and Characteristics
Delta	0.5 to 4 Hz	Restorative/deep sleep, deeply relaxed
Theta	4 to 7 Hz	Deeply relaxed, sleep
Alpha	8 to 12 Hz	Very relaxed, restful, daydreaming, passive attention
Beta	13 to 30 Hz	Awaken state, active, thinking, anxiety, external attention
Gamma	30 to 80 Hz	Perception, memory, attention, concentration, learning

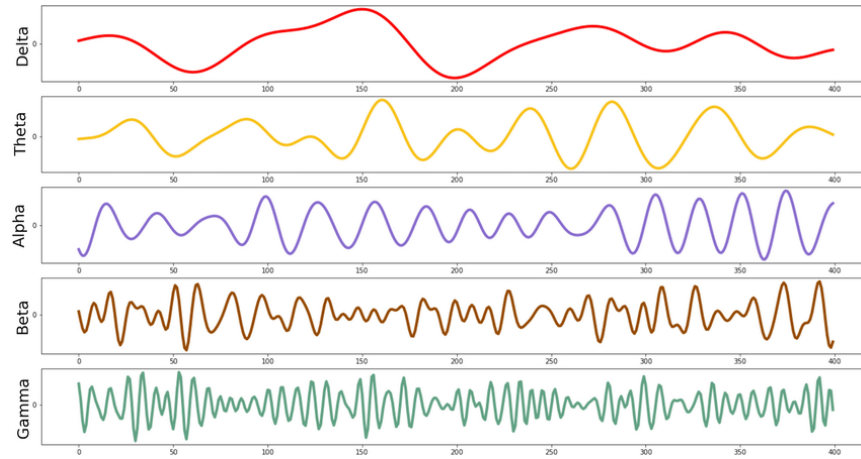


Figure 4: Wave representation of the five EEG rhythms (Extracted from [37]).

2.10. EEG Electrode Placement

In EEG, electrode placement on the scalp is based on standard position systems. The most used one is the 10–20 system shown in Figure 5. In this system, 21 electrodes are used and the distance between them is equal. The electrodes are positioned at locations 10% and 20% from four cranial landmarks: inion, nasion, left and right preauricular points.

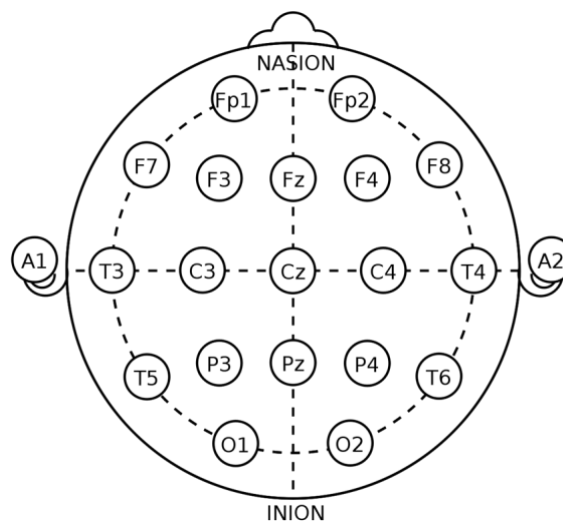


Figure 5: Schematic representation of the EEG 10–20 system (Extracted from [38]).

The 10–10 and 10–5 systems are also used. These result from the addition of electrodes in intermediate positions between those of the initial 10–20 system, which increases the spatial resolution [29], [39], [40].

There is a naming convention for electrode positions. The electrode location starts with one or two characters followed by an odd or even number to indicate the placement on the left or right hemisphere, respectively. The first character concerns the cortical area (F-frontal, C-central, T-temporal, P-parietal and O-occipital). For electrodes within these areas, a second character is incorporated [29].

The 10–20 system is adequate for transcranial brain mapping and for recording evoked and event-related potentials. The 10–10 system is suitable for cases where more detailed EEG data is needed [39], [40].

2.11. EEG Artifacts

EEG signals are used to identify and analyze brain activity. However, signals from other sources beside neuronal activity usually contaminate the signals of interest and add uncontrolled variability to the data. These spurious signals are called artifacts, and reduce the signal-to-noise ratio (SNR) [41]–[43].

EEG artifacts can be classified into two main types: physiological and non-physiological or technical. Physiological artifacts are generated intrinsically by the human body and include eye blink, eye movements, muscular activity, and cardiac artifacts. In contrast, technical artifacts are signals from extrinsic sources such as the EEG equipment and other environment interferences and include line noise, electromagnetic interference and loose electrode contact [41]–[43].

2.11.1. Eye Blink and Movements

Blink artifacts are generated from the muscular movement involved in blinking the eyes. Because this artifact originates at the eyes, it is more evident in the closer forehead channels (specifically Fp1 and Fp2) having, also, some minor influence in other frontal channels [41]–[43].

This artifact has some characteristic properties that facilitate its identification. In the time domain, the electrical potential of a typical eye blink sharply increases and then decreases, within a period of about 250 ms to 300 ms, reaching about a 100 μ V in amplitude. In the frequency domain, it introduces frequency components belonging to the delta and theta EEG frequency bands [41]–[43].



Figure 6: Example of artifacts introduced by eye blinks in EEG data (Extracted from [42]).

Eye movements result from changes in the orientation of the retina and cornea dipole. When the eye moves, the dipole orientation changes and a current away from the eyes and towards the sides of the head is generated. This phenomenon results in a box-shaped deflection with opposite polarity on each side of the head [41]–[43]. In the frequency domain, it contains frequencies belonging mostly to the delta and theta EEG frequency bands. However, it has frequency components of up to 20 Hz [41]–[43].

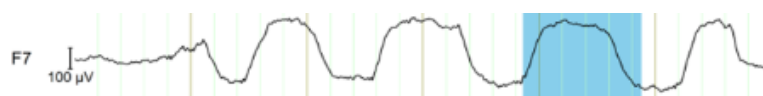


Figure 7: Example of artifacts introduced by eye movements in EEG data (Extracted from [41]).

2.11.2. Non-ocular Muscular Activity

This artifact category includes teeth clenching, talking, sniffing, swallowing, movement of jaw or forehead, as well as shoulder and neck tension [41], [43].

In the time domain, the muscle group involved as well as the degree of contraction and stretch affect the amplitude and waveform of the artifact. In the frequency domain, this artifact is associated with high frequency bands that overlap with the entire EEG spectrum. However, it usually stands out between the 20 Hz and 300 Hz frequency range [41], [43].



Figure 8: Example of artifact produced by muscle activity in EEG data (Extracted from [42]).

2.11.3. Cardiac Artifact

Because of its proximity to the carotid artery, there are pulse artifacts that affect mostly the mastoid area. The arteries located on the head can result in a slight movement of the electrodes because of their pulsation. Also, it is common to find heart electrical activity contaminating the EEG signals [41], [43].

2.11.4. Extrinsic Artifacts

In addition to physiological artifacts there are also extrinsic (non-physiological) artifacts that come from an external source: equipment artifacts and environment artifacts. Equipment artifacts include loose electrode contact and cable movement. Indeed, bad contact between the electrodes and the scalp can result in an unstable signal with slow drifts [41], [43].

There are also environmental artifacts such as line noise or electromagnetic interference from other electronic devices. These have commonly specific associated frequencies of 50 Hz or 60 Hz [41], [43].

2.12. Signal Processing

The EEG data usually cannot be used in its raw form because of the possible existing technical and biological artifacts that contaminate the signals and influence the results. Thus, a preprocessing of the data with the goal to improve the SNR, is required. Several methods can be used to clean and process the signals, as explained below [44].

2.12.1. Independent Component Analysis

The independent component analysis (ICA) is a method for blind source separation used, among other applications, to denoise signals. The ICA model assumes that the measured signal is a linear combination (mixture) of independent non-Gaussian sources, and its goal is to estimate the sources from the measured mixture. To do that, one of the strategies is to maximize the independence underlying the measured data, assuming that there are independent components that are linearly mixed to produce the EEG [44]–[46].

Once the independent components have been segregated, it can be used to identify and remove specific ones corresponding to artifacts in the EEG. Thus, keeping the remaining components intact, the signal can be reconstructed without noise [44].

2.12.2. Filters

Another way to clean the EEG signals is using filters, limiting the signals to frequencies of interest. However, filtering is a compromise between removing noise and losing information of interest, being crucial the use of optimized filter types and parameters.

Usually, scalp EEG comprises signal power mainly in the 1 Hz - 30 Hz frequency band, but the analysis of clinical scalp EEG is commonly performed between 0.5 Hz and 70 Hz, once that range can be clinically significant in certain conditions. Also, signals are affected by the baseline drift (frequencies below 0.5Hz) and powerline noise (frequencies at 50 Hz or at 60 Hz), being necessary to remove these components. To attenuate higher frequencies (> 70 Hz), low-pass filters are suitable. For the noise corresponding to the lower frequency bands (< 0.5 Hz), high-pass filters can be used. Alternatively, a bandpass filter could also be used for the same purpose [34], [47], [48].

A low pass filter cuts off frequencies higher than a certain threshold and maintains the frequencies below this threshold. In contrast, a high pass filter cuts off frequencies lower than a specified threshold and maintains frequencies above this threshold. In addition, a bandpass filter cuts off the frequencies above and below a given frequency band, keeping the frequencies within the band. There is also another type of filter, the notch filter, which cuts off only a narrow band of frequencies, preserving the frequencies higher and lower than the defined notch frequency. The notch filters are suitable for removing specific frequencies, such as the powerline noise at 50 Hz or 60 Hz [48], [49].

According to the filters structure, their impulse response can be classified as Finite Impulse Response (FIR) and Infinite Impulse Response (IIR) filters. A FIR filter is a non-recursive digital filter whose impulse response has a finite duration. This filter does not use previous output values, depending only on the history of the input values. Its main advantage is its stability. On the other hand, a IIR filter is a recursive digital filter with an infinite impulse response. It obtains the output considering the current and previous inputs as well as previous outputs values [50].

2.12.3. Short-Time Fourier Transform

The short-time Fourier transform (STFT) is a sequence of Fourier transforms of a windowed signal and provides both frequency and time information when spectral components of a signal change over time. Therefore, it is used to perform time-frequency analysis on nonstationary

signals, such as the EEG [51], [52].

Time and frequency resolution depend on the window size. To guarantee a good time resolution, small windows should be used, whereas to achieve a good frequency resolution the windows should be bigger [51].

2.12.4. Wavelet Transform

Using wavelet transform, it is possible to decompose the EEG data to analyze the spectral signal changes in time. This method, as the STFT, provides a time–frequency representation of a signal and is able to adjust the time-frequency resolution. It's a time-frequency method for signal analysis that incorporates an adjustable window size [53], [54].

This technique can analyze EEG signals at different scales and analyze very small details, and quick changes in the signals [53].

2.13. Feature Extraction

Feature extraction is one of the most important steps in signal processing since, at this step, relevant information must be identified and extracted from the raw data. The features extracted from EEG data can be divided into several different classes, being the most popular time domain features, frequency domain features, and time-frequency domain features. At a more particular level, entropy-based features are also common in EEG analysis [55].

2.13.1. Time Domain Features

In the time domain, there is a lot of statistical features that can be extracted from a signal, such as mean (mean amplitude of the signal over a specific time period), variance or standard deviation (measurement of the spread of the data), kurtosis (degree of peakedness of the signal distribution) and skewness (measure of the asymmetry of the signal distribution) [50]–[53].

Also, other non-statistical features such as zero-crossing rate (ZCR) are commonly used. The ZCR is defined as the number of times a signal crosses the x-axis and gives an estimation of the main signal frequency using a simple time measure [55]–[58].

2.13.2. Frequency Domain Features

Frequency domain features also include statistical features such as mean, standard deviation, variance, skewness, and kurtosis, that are obtained from the signal in the frequency domain. Other widely used features in the frequency domain refers to relative powers of certain frequency bands. In EEG analysis these bands are delta (δ), theta (θ), alpha (α), beta (β) and gamma (γ), as defined in Table 1. Power ratios between different frequency bands are also used, such as θ/α , β/α , θ/β , γ/δ , $(\theta + \alpha)/\beta$, $(\theta + \alpha)/(\alpha + \beta)$ and $(\gamma + \beta)/(\delta + \alpha)$ [55].

The power spectral density (PSD) is defined as the measure of power distribution over different signal frequencies, providing information about the strength of its different frequency components. PSD can be calculated by parametric and non-parametric methods. Some non-parametric methods used to estimate PSD are Fourier transform, Welch's method or Thompson multitaper method, while some parametric methods include mainly autoregressive (AR) models [55], [59].

2.13.3. Entropy

In past EEG based studies, entropy features have also provided relevant information. Shannon's information entropy, concept first introduced by Shannon in 1948, is a measure of the uncertainty or randomness of a signal and is defined by resorting to the probability distribution values of the observed data [55], [60].

From Shannon's information entropy, there are several derived variations such as, spectral entropy, maximum-likelihood entropy, coarse-grained entropy, correntropy, approximate entropy, sample entropy, permutation entropy, differential entropy and fuzzy entropy [55].

2.14. Functional Connectivity

EEG functional connectivity refers to the evaluation of which and how much brain regions are related over time and is a measure of the statistical relationship between certain physiological signals in time. This method assumes that the synchronization/correlation between brain areas reflects communication between them. In other words, two brain areas are considered part of the same network if their behavior is correlated in a consistent manner [61]–[63].

There are several methods to obtain functional connectivity from EEG data, which in turn can be divided into several subcategories according to some characteristics. Directed or nondirected methods relate to whether they quantify the direction of the interaction. While nondirected functional connectivity concerns only the interdependence between signals, directed methods find statistical causation from the data and allow to discover the direction of the information flow. Other subcategories refer to time domain or frequency domain methods [64].

The most used methods for EEG data analysis are correlation-based methods, coherence-based methods, and phase synchronization methods. Correlation-based methods estimate the linear relationship between two signals, allowing the identification of predictive relationships. Examples of these methods are Pearson's correlation coefficient, Spearman's rank correlation coefficient, cross correlation, and partial correlation. Coherence-based methods measure the linear synchronization between two signals at a specific frequency or frequency band and include, for instance, the magnitude squared coherence, the imaginary part of coherency and the partial coherence. Phase synchronization-based methods measure the consistency of phase relationships between brain areas and identify non-linear functional connectivity. This category includes phase lag index (PLI), phase slope index (PSI) and phase-locking value (PLV) methods [64]–[67].

2.15. Virtual Reality

2.15.1. Definition

Virtual reality (VR) consists of a technology that uses interactive computer-generated graphics to create a simulated environment and give the user an immersive feel of a virtual world. The interactive experience allows the user to explore and interact with the virtual surroundings in a natural and intuitive way [68], [69].

For VR, specialized equipment is used including a headset incorporating a screen and sensors that track the user's head movements. Some VR headsets are also equipped with headphones and hand controllers. These technologies track the user's movements, change the display in real time and provide a combination of sensory cues such as auditory, visual and haptic feedback to create an illusion of reality [68], [69].



Figure 9: Example of a VR system (Extracted from [70]).

2.15.2. VR Applications

Initially, VR technology was used mainly in the gaming and entertainment industries. But now, it also has applications in other areas such as healthcare, aviation, education and scientific

research [68], [69], [71].

Related to healthcare applications and scientific research, VR makes it possible to present emotionally complex stimuli in a controlled manner, and for this reason it has attracted the attention of researchers and psychotherapists in the last years. VR is also being explored for a variety of applications as training medical practitioners, cognitive rehabilitation, physical therapy, helping patients manage pain and anxiety and for the diagnosis and treatment of various pathological conditions. By providing a safe and controlled environment for students and professionals of the health area to train medical procedures, it allows them to reduce patients risk [71], [72].

Also, it has been proved that VR is able to activate the threat-processing circuitry in the brain, and it is already used in the treatment of phobias and post-traumatic stress disorder (PTSD). This is because VR allows the creation of highly realistic and immersive simulations of potentially threatening scenarios in a safe and controlled environment [73].

3. State-of-the-Art

3.1. Related EEG Datasets

It was not found in the literature, EEG datasets concerning situations of unexpected visual threats. There are some datasets involving emotions recognition such as fear and anxiety but none of the datasets are related to an unexpected visual threat situation.

An example of an emotion recognition dataset is SEED-IV. For this dataset [74], video clips eliciting happy, sad, fear and neutral emotions were shown to 15 subjects while EEG signals were being recorded over 62 channels. There are also emotion recognition datasets resulting from VR stimuli presentation, including the DER-VREEG dataset [75] which contains EEG data recorded during VR experiences eliciting different emotions (happy, fear, calm and boredom). In addition, some datasets involving EEG recordings during looming stimuli presentation, such as approaching rotating circles, were also found [76].

However, these datasets are strongly correlated to the emotional response more than to the defensive response resulting from exposure to unexpected visual threats.

3.2. Overview of Related Works

Some studies had explored the brain regions that activate under threatening stimuli. There are studies in humans, marmosets, and some other species. To identify the activated brain areas, some of them use EEG [4]–[6] while others use fMRI [1]–[3], [7]. Regarding the threatening stimulus, most of them resort mainly to images, videos, faces, sounds and to virtual reality videos, all with the aim of representing a threat. Some stimuli involve images and videos of frightening animals or people reacting to threatening scenarios [1], [6], looming visual stimuli [2], [4], [7], exposure to heights [5] and other threatening situations [3]. These studies will be discussed below.

A study conducted by Pichon *et al.* 2011 [1] evaluated if threat defensive responses depend

on attentional control. Participants watched videos of threatening and neutral actions during fMRI scans. The videos consisted of scenes where someone opens a door and could face some threat or not, and diverse threat types were used. To manipulate attention, they performed both a demanding color-naming task and an emotion-naming task. The brain regions found to have increased activity during the threat stimuli were subcortical areas linked to autonomic reflexes and defensive behaviors (the periaqueductal gray and the posterior medial hypothalamus) as well as cortical regions (right lateral premotor cortex, pre-supplementary motor area, bilateral anterior insula and left inferior frontal gyrus). These activated areas were task independent. It was also observed an increased activity in the amygdala when seeing a threatening stimulus together with the emotion-naming task, suggesting that its activation can be modulated by task demands, differing from the other activated regions.

A study conducted by Vagnoni *et al.* 2015 [4] investigated the neural mechanisms by which perceived threat modulates spatiotemporal perception. In this regard, VEPs and evoked oscillatory responses induced by looming visual stimuli were measured by EEG. Participants watched both threatening (spiders and snakes) and non-threatening (butterflies and rabbits) images that expanded in size to simulate approaching and suddenly disappearing. Participants had to imagine the object continuing its route at the same speed and indicate the instant they thought the object would collide with them. It was found a modulation of emotion on VEP components P1, N1 frontal, N1 occipital, EPN and LPP, involving the alpha band, as well as a modulation of speed of approach of stimuli on the N1 parietal, involving the beta band. P1 concerned the left and right occipital–parietal electrodes activity between 115 and 135 ms after stimulus. N1 frontal concerned the frontal electrodes activity between 110 and 135 ms after stimulus, while N1 late parietal concerned the parietal electrodes activity between 150 and 200 m, and N1 late occipital concerned the left and right occipital–parietal electrodes activity between 155 and 185 ms after stimulus. Finally, EPN concerned the occipital–parietal electrodes activity between 200 and 300 ms after the stimulus, and LPP concerned both the central electrodes activity between 400 to 1000 ms after stimulus and between 1400 and 1800 ms after the stimulus. It was also found that threat negatively influences the synchronization over the sensorimotor areas activated by exposure to a looming stimulus.

Fernandes Jr *et al.* 2019 [3] studied how the human brain perceives threats considering a multivariate approach, using fMRI. Here it was studied the brain activation patterns to threatening (man holding a gun) and neutral (man holding a nonlethal object) stimuli, using images, in two different situations: the stimulus being directed towards or away from the participant. The results showed that the perception of the threat moving towards the participant was more intense than the perception of the threat moving away. In the first case, the most activated brain areas were the prefrontal cortex (left inferior frontal gyrus, right subgenual prefrontal cortex, dorsolateral prefrontal cortex, and medial orbitofrontal cortex), the cerebellum, the left putamen, occipital regions (primary visual cortex and the superior, middle and inferior occipital gyrus) and temporal regions (superior, middle and inferior temporal gyrus and Heschl's gyrus). On the other hand, the activations for the stimulus moving away presented high variability between subjects.

In a study on marmoset monkeys, performed by Cléry *et al.* 2020 [7], a looming stimulus was presented during a fMRI scan. Here it was used dynamic visual stimuli (motion in depth) that involve a much more complex analysis by the brain compared to static images. Strong activation was found in regions of the pulvinar, superior colliculus, putamen, parietal, prefrontal and temporal cortical areas, as shown in Figure 10. The activated areas suggest that there is a network responsible for processing visual stimuli approaching the PPS to predict the consequence of these stimuli.

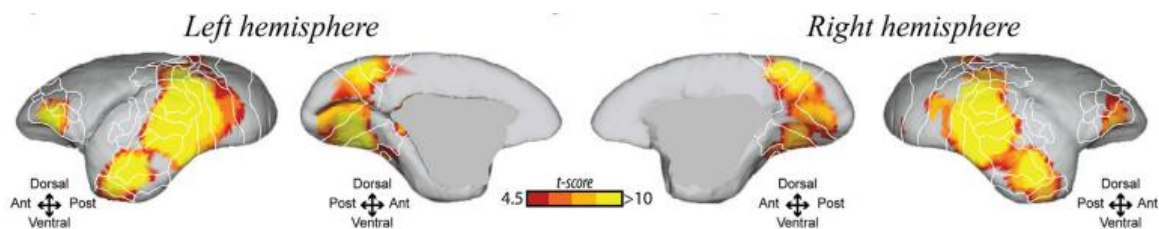


Figure 10: Cortical networks activated by looming visual stimuli in marmoset monkeys (Extracted from [7]).

A study conducted by Gümüş *et al.* 2022 [6] consisted on recording EEG signals while visualizing images from the International Affective Picture System, which represents various

emotions. Specifically, fear-related, and neutral images were used. The event-related potentials (ERPs) and event-related oscillations (ERO) were analyzed. The results from ERP analysis showed that the P7, O1, F3, AF3 and P8 channels (according to the 10-20 electrode position system), were the most discriminative to distinguishing fear and neutral stimulus, and alpha and beta were the most discriminative frequency bands. Significant differences between the neutral and fear stimuli were seen in regions of the parietal, occipital, and frontal lobes of the left hemisphere.

Recently, some studies have also been carried out using VR for stimulus presentation. Balban *et al.* 2020 [5], studied fear responses to visual threats through EEG, behavior, heart rate, skin conductance and respiration. The stimulus consisted of a VR world starting with the scenario of the participant in a laboratory and then transitioning to a threatening stimulus like being attacked by a dog, finding a spider, swimming with sharks or being exposed to heights. It was shown that heights stimulus resulted in robust physiological arousal indicating an increased activation of the sympathetic nervous system. The dogs, spiders and shark stimuli generated more moderated physiological responses. With the aim of evaluating brain areas related to visually driven arousal, intracranial electroencephalography signals (iEEG) were also recorded from a few patients. Patients with insula and orbitofrontal cortex electrodes were chosen once these brain areas are related to emotional regulation and somatic awareness. The results of this experiment showed that low frequency theta activity in the orbitofrontal cortex negatively correlates with physiological arousal resulting from visual threats, while a positive correlation was found for high frequency gamma activity in the insula. Concluding, the orbitofrontal cortex and the insula are strongly correlated with visually driven arousal.

Borst and Gelder 2022 [2] aimed to find which brain regions were involved in threatening and non-threatening stimuli in the PPS using VR during fMRI measurements. The VR scene used consisted of the participant lying in a bed inside a bedroom, and a man entering the bedroom and walking towards the bed in a menacing way. The results of this study indicated that the intraparietal sulcus and the ventral premotor cortex responded more strongly to threatening stimuli entering the nearby space than non-threatening stimuli. Stronger

responses to threat were also found in the right anterior cingulate cortex, left middle frontal gyrus, bilateral extrastriate body area and bilateral cuneus. Additionally, they found that the anterior insula and the amygdala are involved in threat processing. The authors concluded that the interconnected intraparietal and premotor brain areas are related to the tracking of approaching threatening stimuli with the aim of initiating avoidance behavior.

The amygdala seems to be one of the brain regions most found in threat processing research. In fact, it has been shown that the process of detecting threatening stimuli involves the diverse human senses and several pathways to the amygdala with the involvement of cortical and subcortical areas. When considering a conscious situation of evaluation of a potentially threatening stimulus, a cortical pathway has been discovered. In this pathway, the visual information goes from the thalamic lateral geniculate nucleus to the primary visual cortex and finally to the amygdala. On the other hand, when considering a situation of fast and automatic response to a threatening stimulus, it was identified a direct pathway that reaches the amygdala without the involvement of the primary sensory cortices. A subcortical pathway involving the superior colliculus, the thalamic pulvinar and the amygdala has been proposed to mediate a rapid visual analysis of potentially threatening stimuli through the visual sensory input [77], [78].

4. Materials and Methods

This chapter describes all the materials and methods employed throughout the experimental work, including the VR video development and preparation, the brain activity acquisition through EEG, signal processing, feature extraction and statistical analyses.

4.1. Experiment Development

The scheme presented in Figure 11 summarizes the steps of the general experimental setup, which are detailed in the subsections below.

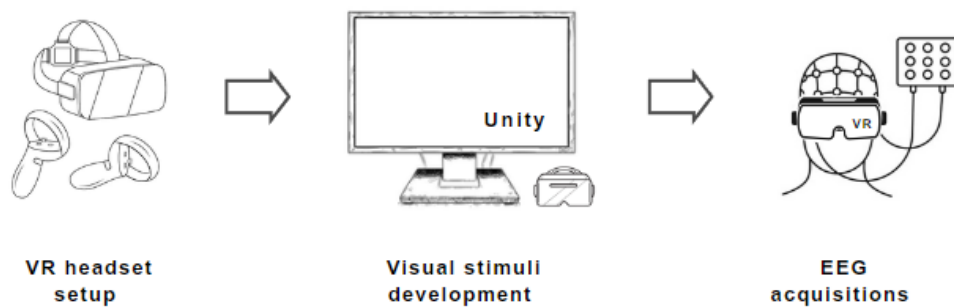


Figure 11: Scheme of the general experimental setup steps.

As represented in the scheme, there are three main steps in this phase: the setup of the VR headset, the development of the visual stimuli (VR video) to be displayed in the headset and, finally, the acquisition of EEG data during the presentation of the previously developed VR video to several volunteers.

4.1.1. Virtual Reality Equipment

In this study, the visual stimulus was developed using VR. For that, a VR headset (Reverb G2, HP, Palo Alto, California) comprising lenses, headphones and hand controllers was used.

This headset is shown in Figure 12.

The VR headset was connected to a general-purpose computer, and the Mixed Reality Portal application [79], also used to select and play the VR video (visual stimulus), allowed the initial required setup of the VR space.



Figure 12: HP Reverb G2 headset (Extracted from [80]).

4.1.2. Visual Stimulus

A VR video (visual stimulus) was created recurring to Unity software, which is a real-time development platform for creating interactive two-dimensions (2D), three-dimensions (3D), virtual reality (VR) and augmented reality (AR) experiences. This platform includes assets (files), through which it is possible to create diverse and elaborate scenarios. Assets can be 3D models (objects), textures (applied to the surfaces of 3D models to give them color and details), materials (define objects appearance by connecting textures and other properties such as lighting and shininess), audio files (sound effects and background music) and scripts (programs written in C# that control the objects behavior).

The VR video developed consists of a calm scenario of a forest at dusk lighting conditions and containing typical elements such as trees, flowers and grass, as well as light breeze movements (Figure 13.a). The video also includes a background forest sound. It should be noted that the goal was to create a scenario as calm as possible and with the fewest possible

distractions so that a minimum of other brain activity unrelated to the stimulus would be detected. The scene is presented as if the observer were walking straight ahead along the forest path.

The video lasts 5 min and 35 s and at 2 min and 3 s the threatening stimulus appears (Figures 13.b and 13.c). The threatening stimulus consists of an unexpected rock coming towards the viewer that ends up obscuring the scene and then disappears. The rock is accompanied by a crashing sound. It should be noted that, although the goal was to study the brain activity because of the appearance of a visual unexpected threat (that is, the rock), introducing a mute stimulus did not elicit a defensive reaction. After the threat stimulus, the scene continues along the forest path.

To identify whether the participant's reaction to the threat stimulus and the associated brain activity relate to defensive mechanisms or just to sensory inputs, two additional stimuli were introduced. To account for the effect of the crashing sound that accompanies the threat stimulus and to segregate its effect from the visual part, at 3 min and 14 s, the same sound was reproduced, but this time without the visual stimulus, that is, without the rock. Also, at 4 min and 45 s, a small bird crosses the scene (Figure 13.d), representing a neutral visual input.

Figure 14 shows a diagram of the VR video timeline and the instants in which the mentioned stimuli appear.

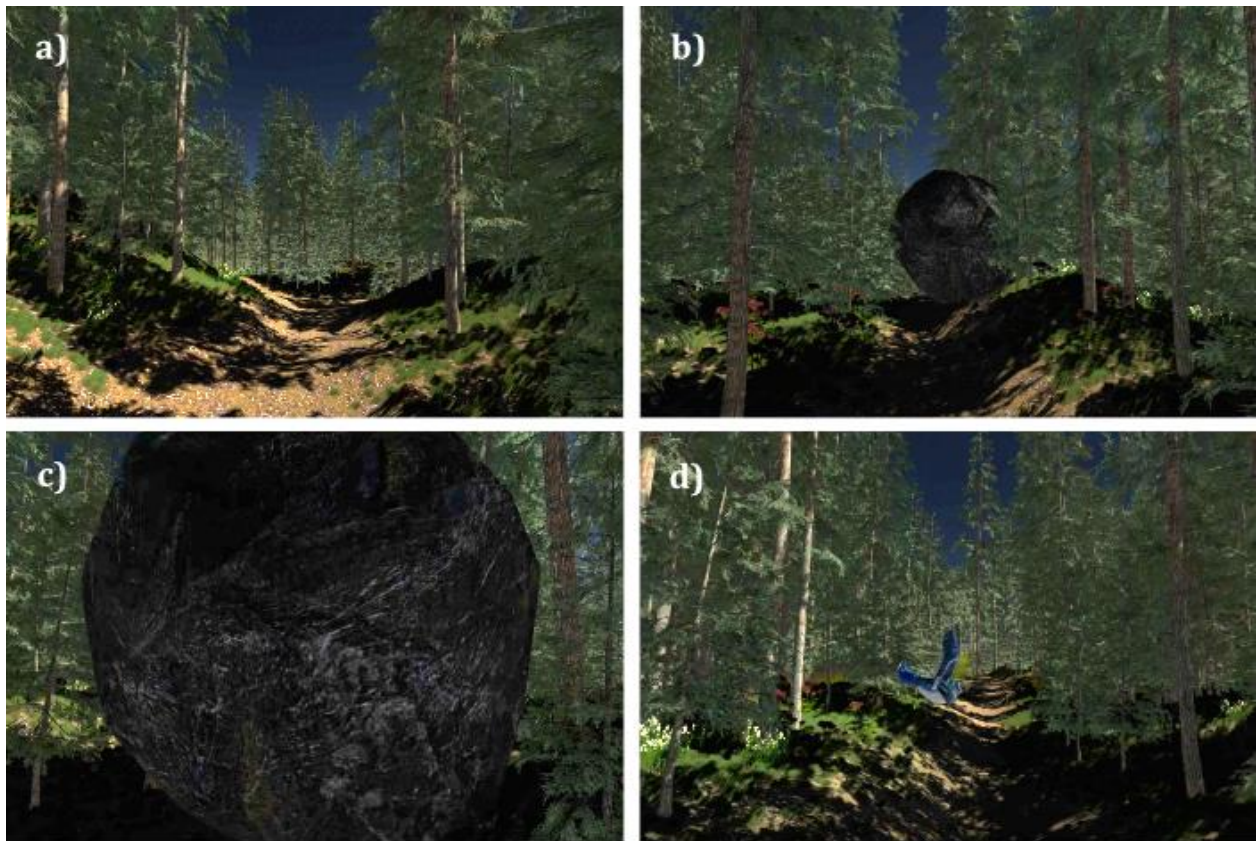


Figure 13: Example of four frames of the developed VR video; a) presents a neutral part of the video; b) and c) present the moment of the rock appearance ; d) shows the moment of the bird appearance.

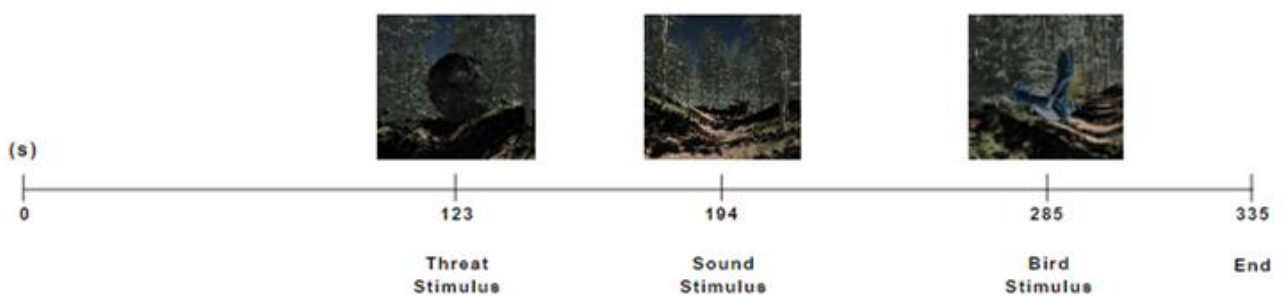


Figure 14: Video timeline with the instants of the three presented stimuli.

Before proceeding to the recruitment of participants, diverse video versions were developed, and their effects were verified by the research team. The final characteristics,

mentioned above, were the most favorable to elicit the desired effect (defensive reaction).

The selection of the video's frame rate was also carefully considered since, as mentioned in section 2.6, the visual stimulus needs to be presented for at least 13 ms to be detected by the observer (i.e. a frame rate equal or lower than 75 fps). So, since it was the frame rate value provided by Unity that produced the best image quality in the final video, a frame rate of 24 fps was selected. It should be noted that all frame rate values available on Unity and lower than 75 fps were tested with the aim of obtaining a final video with the best possible image quality.

The video was recorded in Unity in 360° view mode, with a frame dimension of 8192 by 4096, and in ProRes QuickTime format [81], being later converted to WebM format [82]. This format conversion was necessary to provide the best results in terms of overall video quality in the VR headset.

After several experiments, these were the frame rate, resolution and video format that provided the best image quality when the video was displayed in the VR headset.

4.1.3. EEG Acquisition System and Electrode Placement

To acquire the participant's brain activity, the recorder device (LTM-EU, Micromed, Treviso, Italy) together with the SystemPLUS Evolution software [83] were used. It was also used the electrode cap (Electro-Cap International, Eaton, Ohio, United States) (Figure 15), since it provides an easier and faster technique for placing EEG electrodes. The EEG cap is composed of an elastic fabric with pure tin electrodes embedded on it and positioned according to the international 10-20 electrode placement system.



Figure 15: NeuroEvolution International (Extracted

EEG Electro-Cap from [84]).

In this experiment, 19 channels were used, including Fp1, Fp2, F7, F3, Fz, F4, F8, T3, C3, Cz, C4, T4, T5, P3, Pz, P4, T6, O1 and O2, and signals were acquired at a sampling frequency of 512 Hz.

4.1.4. Stimulus and EEG Recording Synchronization

To guarantee the synchronization of the beginning of the video with the EEG signal acquisition and, therefore, to know exactly the instants of the acquired signal corresponding to the different stimuli of the video, a Python program was developed. This program saves, in a text file, the exact time (in milliseconds) the video was started pressing the left mouse button. It runs in the background and saves the time whenever the left mouse button is pressed.

On the other hand, from the EEG saved file it is also possible to access the exact start time of that EEG recording, making it possible to find the EEG data corresponding to specific instants of interest of the video.

4.1.5. Participants and Ethical Aspects

The study protocol was approved by the Ethics committee of the Faculty of Medicine of the

University of Coimbra under the protocol CE-017/2023.

The inclusion criteria consisted of young adults with ages between 18 and 40 years old. The exclusion criteria consisted of visual deficits, neuropathological conditions, cardiac pathologies and use of neuropharmaceuticals. No further gender, social or educational conditions were considered.

At the acquisition date, the participants were informed about the study procedures, but without information about the video content. A copy of the informed consent (Annex 1) was given, and they had time to read and clarify any doubts. If they agreed to participate, and the inclusion/exclusion criteria were met, they had to sign two copies of the informed consent, one to keep with them and the other to the research team.

After the EEG data recording, participants were also questioned about the video effect. No personal information besides the needed for depicting inclusion/exclusion criterion was collected. Related to confidentiality and data protection, each participant was identified with a numerical code to keep their identity inaccessible in further data analysis or publications.

The study included 26 eligible volunteers, and the associated data is given in Annex 2.

4.1.6. Procedure

The involvement of each participant in the study contemplated only one day/session, where the participant was connected to an EEG system to record brain activity while simultaneously viewing the VR video through the headset. The whole procedure took about one hour, and no posterior follow up was required.

After signing the informed consent, the experimental phase was initiated. First, the scalp regions corresponding to electrode positions were cleaned using an exfoliant and alcohol and then the electrode cap was placed. Gel was then introduced into each of the cap electrodes using a syringe. Finally, the VR headset was placed over the EEG cap, as presented in Figure 16. During this procedure, participants were comfortably seated in a chair. Before starting the EEG register, they were instructed to stay as still as possible, do not talk and to stay calm during the video visualization.

Ultimately, the equipment was disconnected, and participants were asked about their personal experiences while watching the video. I was asked if they observed the threat stimulus and if they felt threatened by it.



Figure 16: Example of a participant along the experimental procedure, with the EEG cap and VR headset connected.

4.2. Signal Processing

The scheme presented in Figure 17 summarizes the steps performed in the signal processing phase, which are detailed in the subsections below.

These steps were implemented using the MATLAB programming language, and the code can be found in <https://github.com/CarolinaLopes00/Threat-Brain-Activity.git>.



Figure 17: Scheme of the signal processing steps.**4.2.1. Remove Excess Data**

The EEG recordings were initiated some minutes before starting the video projection and were finalized some minutes after the video ended. Being so, it was necessary to remove the initial and final time instants of recordings, ending up with EEG files lengths corresponding to 5 min and 35 s (the same duration of the VR video). This was performed using the start time instants of the EEG recordings, and the start time of the video, obtained as described in section 4.1.4. Some main characteristics of the EEG recorded data are summarized in Table 2.

Table 2: Characteristics of each EEG file.

Characteristic	Value
Length	5 min and 35 s
Sample rate	512 Hz
Number of channels	19
Number of data points	171520
Time resolution	0.002 s

Accordingly, each EEG file is a two-dimensional array with the rows concerning the time instants and the columns, the EEG channels.

4.2.2. Filtering

The frequency range of interest was considered between 0.5 Hz and 80 Hz. Therefore, to obtain that frequency range and remove noise components that influence the signals, it was necessary to apply filters to the EEG data. Two types of filters were applied: notch filters and a bandpass filter.

A IIR notch digital filter of second order was applied to exclude the frequency component of 50 Hz, concerning the powerline noise. Additionally, a second notch filter was applied at 37 Hz since this frequency component was also evident in the signal spectrum. For these purposes, the *iirnotch* MATLAB function was used.

To eliminate the lower (< 0.5 Hz) and higher (> 80 Hz) frequencies, the data was bandpass filtered, applying a FIR band-pass digital filter using the *bandpass* MATLAB function. This function designs a minimum-order filter. Also, it compensates for the delay resulting from the filter application, returning the output with the same dimensions as the input.

4.2.3. Artifacts Removal

The next step consisted of removing the remaining artifacts, namely eye blinking, eye movements, muscular activity, and cardiac artifacts. For this, ICA was applied.

The number of computed independent components was the same as the number of EEG channels, that is, 19. The analysis of the component's characteristics in the time domain as well as their spectral content allowed us to identify the artifacts among all the obtained independent components. The identified components related to artifacts were then eliminated, and the EEG was reconstructed without them. It is expected that the reconstructed EEG should present better quality than the original one, given the presence of artifacts in the original EEG.

4.2.4. Feature Extraction

The last processing step consisted of extracting features from the filtered data. For this purpose, for each EEG channel, the relative PSD values were obtained for each frequency band:

delta (0.5 to 4 Hz), theta (4 to 7 Hz), alpha (8 to 12 Hz), beta (13 to 30 Hz) and gamma (30 to 80 Hz). To compute the PSD values, the signals were segmented into overlapping windows of 1 s with an overlap of 50%, using a Hamming window. For this, the *spectrogram* MATLAB function was used. This function, in addition to returning the STFT of signals, also returns the PSD values for each time segment and frequency value. Then, for each segment, the PSD value related to each frequency band was computed by adding all the PSD values corresponding to the frequencies included in each band. Finally, the relative PSD value for each band resulted from dividing the PSD values obtained for each band by the sum of all the PDS values.

Therefore, 95 features were obtained, corresponding to each frequency band (5) and each EEG channel (19).

4.3. Identification of Relevant Brain Areas

The next step concerns the discovery of the relevant brain areas, that is, the activated brain areas during a threatening situation. With the purpose of discarding activations associated with other phenomena than the threat situation, the activated brain areas for the other two stimuli described in section 4.1.2 (crashing sound and bird stimuli) were also obtained. In the end, the activations found for each of the three stimuli were compared.

The code concerning the implementations described below can be found in <https://github.com/CarolinaLopes00/Threat-Brain-Activity.git>.

4.3.1. Data Distribution Test

Firstly, the One-sample Kolmogorov-Smirnov test was applied to the relative PSD values of each frequency band and of each EEG channel of all the participants, to find if the data followed a normal distribution. This step is necessary to choose the appropriate statistical test used to posteriorly discover the relevant brain areas.

4.3.2. Statistical Significance Test

The subsequent step consisted of finding the relevant EEG channels. A channel is considered relevant if the data associated with it (that is, the relative PSD values) exhibits significant differences between the neutral state and the stimulus state, where the neutral state corresponds to a time interval of the video without stimuli and the stimuli states correspond to the time intervals starting at the beginning of each stimulus (considering the three applied stimuli: threat, sound and bird). In this step, it is determined which channels and which frequency bands are significant. For this, the Kruskal-Wallis nonparametric multiple comparison test was applied.

Related to the time window without stimulus (neutral condition), instead of considering just one random neutral second of the video, it was used the average of the neutral part of the video before the appearance of the first stimulus, between the 20 s and 100 s, aiming to reduce variability in the neutral condition. Regarding each of the stimuli, instead of just one post-stimulus window, several consecutive post-stimulus windows were analyzed to take into account the total duration of the stimuli, as well as possible delays on reaching the different brain areas. The consecutive instants have a 50% overlap. Table 3 presents the post-stimuli time-windows analyzed for each of the stimuli.

Table 3: Post-stimuli time-windows analyzed for each of the stimuli.

Condition	t (stimulus)	t (stimulus+1)	t (stimulus+2)	t (stimulus+3)
threat stimulus	122.5 s - 123.5 s	123 s - 124 s	123.5 s - 124.5 s	–
crashing sound stimulus	193.5 s - 194.5 s	194 s - 195 s	194.5 s - 195.5 s	–
bird stimulus	285.5 s - 286.5 s	286 s - 287 s	286.5 s - 287.5 s	287 s - 288 s

Since the bird stimulus takes longer than the threat and sound stimuli, an additional post-stimulus instant is considered for this case.

In this manner, for each of the three stimuli separately (threat, crashing sound and bird), a multiple comparison through the Kruskal-Wallis test was conducted among the PSD data concerning the neutral condition and each of the consecutive post-stimulus time windows described in Table 3.

Figure 18 schematizes the comparison process applying the Kruskal-Wallis test to the mentioned instants. The instants that present significant differences compared to the neutral state are marked in red in the figure at the right. This figure results from the application of the Kruskal-Wallis test in MATLAB.

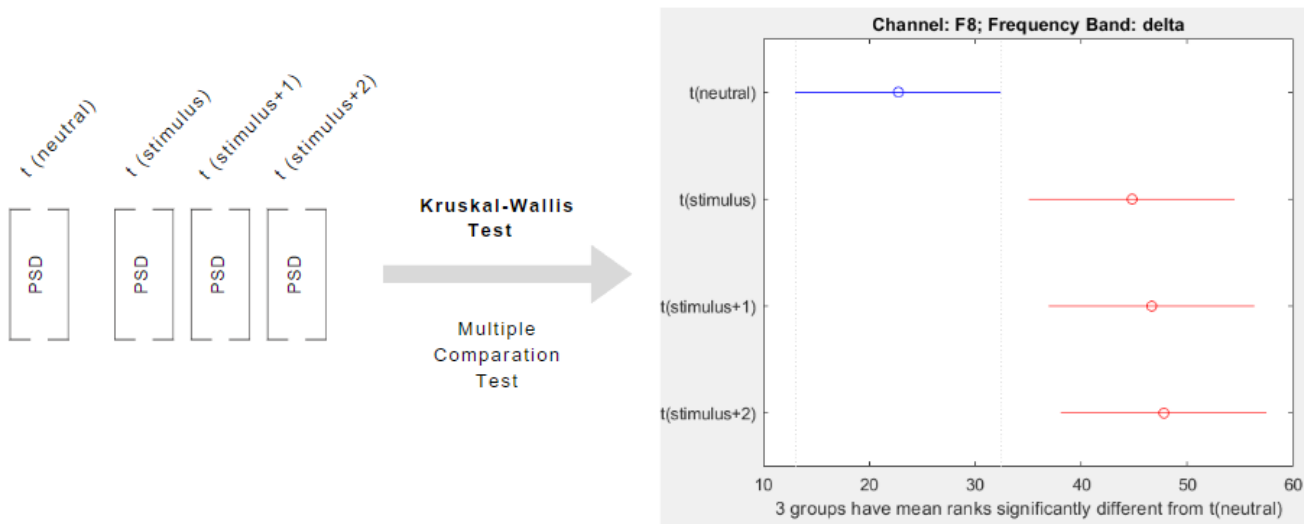


Figure 18: Example of the Kruskal-Wallis test for the F8 delta band and for the threat stimulus case.

As the number of performed statistical tests increases, the probability of a type I error (false positive error) also increases. Therefore, during the multiple comparison tests, a multiple comparison correction using the Bonferroni method was applied. The Bonferroni method is a conservative approach commonly employed as a post-hoc test in several statistical analyses to adjust the probability values (p-values) when conducting multiple statistical tests. Under a significance level α (5 % for the present case), this method rejects each hypothesis if its probability of error is less than α/n , where n represents the number of hypotheses being tested

[85], [86].

As mentioned before, the activated brain areas found for each of the three stimuli separately were compared to discard activations unrelated to the threat situation. Therefore, if the same frequency band of the same EEG channel is found for the threat stimulus and for one of the other two stimuli, it is excluded and considered insignificant for the threat stimulus. Thus, only the frequency bands and EEG channels found as significant exclusively for the threat stimulus are considered.

It should be noted that, of the twenty six participants, six did not react or felt threatened by the stimulus and were excluded from the analyses, once including them could bias the results. However, the data from these six participants were posteriorly used to perform additional analysis to corroborate the relevant brain areas and frequency bands obtained for the threatening situation. This way, the same significance analysis first performed with the twenty participants who felt threatened, was also performed using only the six participants who did not feel threatened by the stimulus. The objective of this analysis was to obtain the relevant features (brain areas and frequency bands which exhibit significant differences between the neutral and the threat stimulus states) for the case of the group of participants who did not feel threatened and compare them with the results obtained for the group who actually felt threatened. Features found in both the analysis with the twenty participants who felt threatened and in the analysis with the six participants who did not feel threatened are not considered relevant to a threatening situation.

4.4. Functional Connectivity Between Relevant Brain Areas

After obtaining the brain areas activated because of the threatening stimulus, the next step was to find the connections between these areas, as well as the strength of these connections. This later allows to obtain the brain network representative of a defensive reaction to a threat. For this, five methods of functional connectivity were implemented in MATLAB: coherence (COH), imaginary part of coherence (iCOH), weighted phase lag index (wPLI), mean phase

coherence (MPC) and direct transfer function (DTF). The COH, iCOH, wPLI and MPC methods are used to find the significant connections while the DTF method is used to find the direction of those significant connections. These methods are described in the next subsections, and their implementation can be found in <https://github.com/CarolinaLopes00/Threat-Brain-Activity.git>.

Two concerns taken into account for the connectivity analysis of EEG data are the volume conduction and SNR problems. The volume conduction problem refers to the activity of a source being present in more than one EEG channel, and a channel reflecting the activity of multiple neuronal sources. There's also the SNR problem since signals reflect a mixture of the signal-of-interest, corresponding to the activity of the neuronal population of interest, and noise. Consequently, aiming to obtain connectivity patterns that reflect genuine neuronal interactions, two connectivity methods capable of overcoming these problems were included in the analysis: iCOH and wPLI [64], [87].

For each connectivity method (COH, iCOH, wPLI and MPC), the connectivity values for each channel pair were evaluated for two conditions: neutral state (pre stimulus) and threat stimulus state (post stimulus).

To reduce variance within the neutral state, the connectivity was calculated for the time series data corresponding to each individual second of the interval comprehended between 20 s to 100 s (corresponding to a neutral part of the video), and then the resultant connectivity values were averaged. Regarding the threat stimulus state, the associated connectivity values were obtained for the time series data corresponding to the instant of the threat appearance on the video, which corresponded to the 122.8 s - 123.8 s time window. The connectivity values for each channel pair were stored in three matrices containing the average of these values across participants: one for the neutral state (pre-stimulus), one for the threat stimulus state (post-stimulus) and one for the difference between the connectivity values of the stimulus and the neutral states (pos-pre). It is important to analyze the matrix of the difference of connectivity values between the threat stimulus state and the neutral state, because a connection associated with a high connectivity value in the stimulus state may not necessarily indicate that this connection is relevant in the threat situation since this connection can also

present a high connectivity value in the neutral state. Thus, analyzing the difference matrix makes it possible to highlight the connections that are really relevant in the stimulus state in comparison with the neutral state.

Once the connectivity for each pair of channels and for each condition was obtained, a statistical test was applied to the values obtained for each participant in order to assess the significant differences between the connectivity of the neutral and the threat stimulus states, aiming to find the channel pairs with significant connections induced by the threat. Before that, the One-sample Kolmogorov-Smirnov test was applied to the connectivity values to find if the data followed a normal distribution. The test decision, considering a significance level of 5%, indicated that data did not follow a normal distribution. Therefore, the Kruskal-Wallis nonparametric test was then used to assess the significant differences between the connectivity of the neutral and the threat stimulus states, considering a significance level of 5%. A multiple comparison correction was also performed in these results and two correction methods were considered: Holm-Bonferroni and a less conservative method, false discovery rate (FDR). After obtaining the channel connections that presented significant differences between the two states, only the connections with higher connectivity values for the threat state than for the neutral state were considered since these are the ones that correspond to an increase in connectivity induced by the threat stimulus. To obtain more reliable results, only the statistically significant channel connections that were present in at least three of the four connectivity methods were considered relevant. But since this approach resulted in almost no significant connections for each method, a new approach was considered: the same Kruskal-Wallis test but considering a smaller significance level of 1% and with no multiple comparison correction. Although this new approach resulted in a slightly larger number of significant connections for each method, this number remained very small and only one connection was found in common with at least three of the four connectivity methods. Because of this, it was decided to use a different approach without resorting to statistical tests. This final approach consisted of using the matrix of the difference values between the connectivity values of the threat stimulus state and the neutral state (pos-pre) of each connectivity method. To compare the results of all the methods and to obtain the connections in common with at least three of

them, only the difference values higher than a threshold corresponding to the 0.65-quantile (that is, the value above which 35% of the difference values are), for each method, were considered relevant. The choice of the threshold started with higher values but, in the end, the 0.65-quantile was chosen because a threshold above this value resulted in few connections in common with at least three of the four methods.

The next step consisted of discovering the direction of the obtained connections, that is, the direction of the information flow between the areas of those connections. This allows to obtain a brain network representative of a defensive reaction to a threat. In this sense, the DTF directed connectivity method was applied to the threat stimulus EEG data (Pos Stimulus) to discover the direction of each of the previously found significant connections. The threat stimulus data was the same used for the other connectivity methods (corresponding to the 122.8 s - 123.8 s time window), and a DTF matrix containing the DTF values of each channel pair averaged for all the participants was obtained.

4.4.1. Coherence and Imaginary Part of Coherence

COH is a nondirected frequency-specific functional connectivity method once it is a measure of linear synchronization between two signals at a specific frequency or frequency band. This method measures the consistency of phase synchronization between two signals, that is, how the signal phases are coupled to each other [64], [67].

If $X_i(f)$ and $X_j(f)$ represent the complex Fourier transforms of the time signals $\hat{x}_i(t)$ and $\hat{x}_j(t)$ of channels i and j , respectively, then the cross spectral density between i and j is defined as:

$$S_{ij}(f) = X_i(f)X_j^*(f) \quad (1)$$

and, consequently, the normalized cross-spectrum is:

$$C_{ij}(f) = \frac{S_{ij}(f)}{(S_{ii}(f)S_{jj}(f))^{1/2}} \quad (2)$$

Finally, coherence is defined as the absolute value of the normalized cross-spectrum:

$$COH_{ij}(f) = |C_{ij}(f)| \quad (3)$$

On the other hand, the imaginary part of coherence concerns only the imaginary part of the normalized cross-spectrum $C_{ij}(f)$, and it is obtained by the projection of the complex normalized cross-spectrum onto the imaginary axis [64], [87]:

$$iCOH_{ij}(f) = \text{Imag}(C_{ij}(f)) \quad (4)$$

By excluding the real axis contributions, this method excludes instantaneous interactions that could result from field spread, once this problem strongly affects the real part but not the imaginary part [64], [87].

Both COH and iCOH values range from 0 to 1, with 1 representing high connectivity.

4.4.2. Weighted Phase Lag Index

wPLI is a nondirected functional connectivity method which measures how the phase angle differences between two signals are distributed towards positive or negative parts of the imaginary axis. Volume conduction is the principal cause of 0° or 180° phase differences between signals and this method accounts for this effect. The wPLI is a weighted method since it scales contributions of angle differences based on their distance from the real axis. It is obtained from the imaginary part of the cross spectral density S_{ij} and it is defined as [66], [88]:

$$wPLI = \frac{\sum_{t=1}^n |imag(S_{ij,t})| sgn(imag(S_{ij,t}))}{\sum_{t=1}^n |imag(S_{ij,t})|} \quad (5)$$

This method weights the cross spectral density regarding the magnitude of the imaginary component which attenuates the influence of cross spectral density elements around the real axes [66], [88].

This method also ranges from 0 to 1, with 1 representing full connectivity.

4.4.3. Mean Phase Coherence

MPC is a nondirected functional connectivity method that measures the phase synchronization between signals. It uses the instantaneous phase values of the signals, obtained from the Hilbert transform $s(t)$, to calculate the phase difference ϕ . The instantaneous phase of a signal $s(t)$ is defined by Equation 6 [89].

$$\phi(t) = \arctan \frac{s(t)}{s(t)} \quad (6)$$

Posteriorly, the MPC is then obtained from Equation 7 [89]

$$MPC = \left| \frac{1}{N} \sum_{j=0}^{N-1} e^{i\phi(j\Delta t)} \right| \quad (7)$$

This method also results in values ranging from 0 to 1, with 1 corresponding to full connectivity [89].

4.4.4. Directed Transfer Function

DTF is a directed connectivity method since it also quantifies the direction of the interaction. In other words, having channels i and j , DTF describes if the information flow is from channel i to j or from channel j to i . This method estimates connectivity based on a multivariate autoregressive model (MVAR), providing robustness regarding noise, which makes DTF a suitable method for neuronal signal connectivity estimates [90].

Resulting in values from 0 to 1, it describes the ratio between the inflow of information from channel j to i and all the inflows to channel i , as described in Equation 8 [90].

$$DTF_{j \rightarrow i}(f) = \sqrt{\frac{|H_{ij}(f)|^2}{\sum_{k=1}^k |H_{ik}(f)|^2}} \quad (8)$$

In Equation 8, k is the number of channels and $H_{ij}(f)$ is the transfer matrix [90].

$DTF(i,j)$ describes the causal influence of channel j on channel i . A high $DTF(i,j)$ value indicates a strong connectivity from channel j to channel i . That is, if $DTF(i,j)$ is higher than $DTF(j,i)$, it means that the information flow is from channel j to channel i .

4.5. Frequency Bands Connectivity Analysis

The connectivity analysis carried out previously encompassed the entire spectrum of the signals, that is, the entire frequency band from 0.5 Hz to 80 Hz. In the next step, the goal was to perform a frequency-specific connectivity analysis, that is, for each frequency band separately. For this purpose, the COH method was applied once it measures linear synchronization between two signals at a specific frequency or frequency band. Thus, the COH values were calculated for each frequency band separately, and for each pair of channels and each condition

(pre-stimulus, post-stimulus and post-pre (difference between the stimulus and the neutral states)). For this analysis, the post-pre matrices, composed of the average values between participants, were used.

5. Results and Discussion

5.1. Preliminary Visual Analysis of Extracted Features

To obtain a notion of the results before performing the previously mentioned analyses, some preliminary visual analyses were carried out.

First, spectrograms were obtained for each participant and channel. The spectrograms show the PSD values of each time segment and each frequency and were created with windows of 1 second and with 50% overlap. The segments were windowed using a Hamming window.

Figure 19 represents an example of one of the obtained spectrograms.

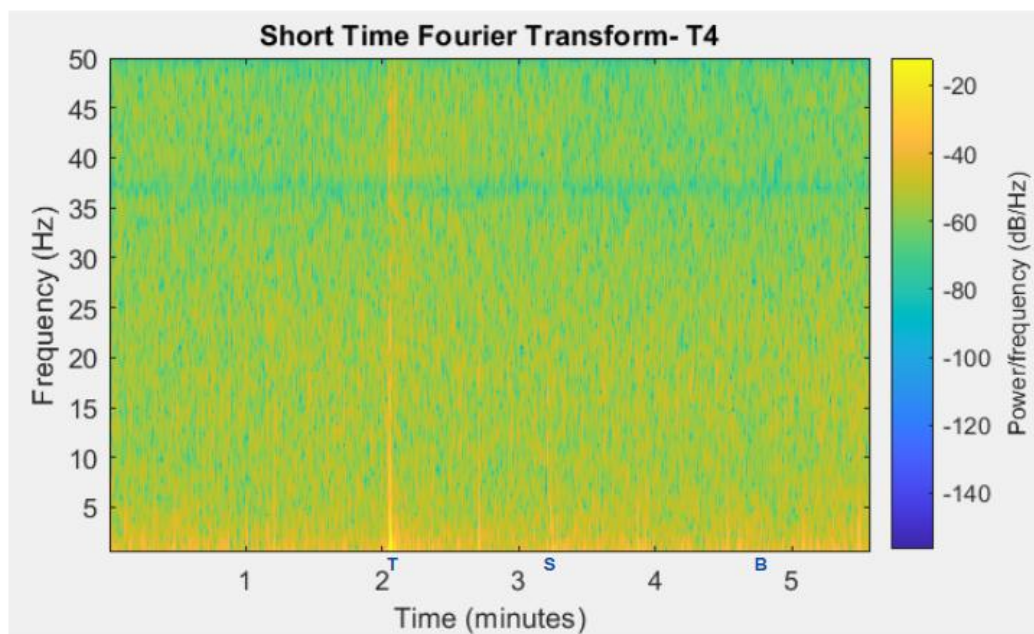


Figure 19: Example of a spectrogram for channel T4, where T, S and B represent the instants of the threat, sound and bird stimuli, respectively.

Observations among participants evidenced an increase in the PSD values at the threat stimulus instant (marked with T) compared to neutral instants, which was a promising indicator for the future analyses. On the other hand, this effect was rare for the instants of the crashing sound and bird stimuli, once, in general, no meaningful differences were observed between the PSD values of each of these stimuli instants and the neutral instants.

Then, boxplots were created for each frequency band, channel, and stimulus, englobing the relative PSD data of all the participants. In Figure 20 is an example of the boxplots obtained for the threat stimulus, and for the beta band of the same channel (T4 channel) presented in Figure 19.

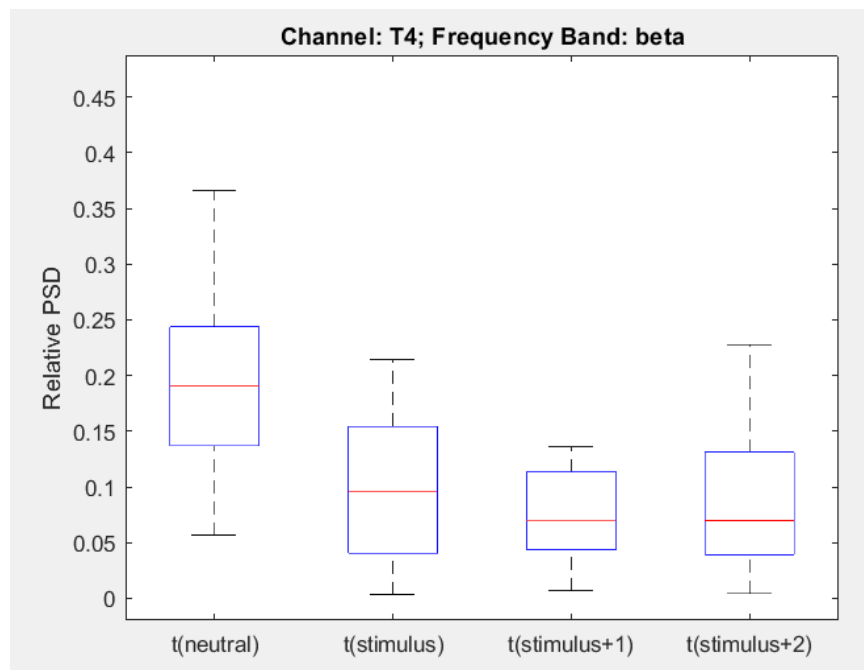


Figure 20: Example of the boxplots for the beta band of channel T4, for the threat stimulus. Each boxplot represents one of the four time instants: $t(\text{neutral})$, and $t(\text{stimulus})$, $t(\text{stimulus}+1)$ and $t(\text{stimulus}+2)$ which represent the three consecutive instants immediately after the threat stimulus appearance, as described in section 4.3.2.

In the example of Figure 20, it is also possible to observe a significant difference between the relative PSD values of the neutral instant and the values of the instants corresponding to the stimulus, once no overlapping of boxplots were evidenced between the neutral and threat stimulus instants. This is in line with what was observed in the spectrogram for the same channel presented in Figure 19.

As with the spectrograms analysis, this boxplot analysis also allowed a previous and global idea of the results, since it was observed, for some frequency bands of some channels, significant differences between the relative PSD values of the neutral and the threat stimulus state. In these boxplots analyses, there was also not much evidence of significant differences between the neutral instant and the crashing sound and bird stimuli instants.

5.2. Relevant Brain Areas

5.2.1. Results

After applying the One-sample Kolmogorov-Smirnov test to the relative PSD values of each frequency band and of each EEG channel of all the participants, considering a significance level of 5%, it was discovered that the data did not follow a normal distribution. Because of that, the Kruskal-Wallis nonparametric multiple comparison test was applied.

Performing the Kruskal-Wallis test, the features that exhibited significant differences between the neutral state and the stimulus state, for each of the three stimuli, were obtained. The results were corrected from multiple comparison effect by the Bonferroni method, and are presented in Table 4.

Table 4: EEG channels and frequency bands that presented significant differences between the neutral state and each of the 3 stimuli, using a significance level of 0.05.

Threat	Sound	Bird
T5- beta, alpha, delta	T4- theta	T4- theta
T4- beta, delta	Cz- beta	F8- beta
Cz- beta	F8- beta, delta	
C3- gamma, beta, delta		
T3- gamma, delta		
F8- gamma, beta, delta		
Fz- beta		
F7- gamma, delta		
Fp2- gamma		
Fp1- beta, delta		

5.2.2. Relevant Threat Brain Areas and Frequency Bands Discussion

As seen in Table 4, regarding the threat stimulus, the following relevant channels were obtained: T5, T4, Cz, C3, T3, F8, Fz, F7, Fp2 and Fp1. Significant differences were observed in almost all the consecutive post-stimulus time windows compared to the neutral window, and not just in the first post-stimulus window. Although some hypotheses are presented below to better explore the activation of these areas as response to threat stimulus, it is important to remark that the brain activity involves highly complex mechanisms that cannot be completely explored by EEG analysis.

Regarding the T5 channel, it is located near the left associative visual cortex or left inferior lateral occipital cortex, responsible for a complex processing of visual information. This area processes information concerning spatial orientation, depth perception, location and movement of objects in space and objects recognition, which is received from the extrastriate

cortex [91]–[94]. These functions have a direct relation with the visual recognition of the threatening stimulus presented in this study, once the stimulus represents an object that appears unexpectedly in the scene.

T4 channel is near the right primary auditory cortex, located on the superior temporal gyrus. These areas are responsible for complex language and auditory processing once they process sound and comprehension of speech. The activation of this auditory processing area is expectable because of the sound that accompanies the threatening stimulus. However, this area is also activated when only the sound stimulus or the bird stimulus (without sound) are presented but at different frequency bands. Being so, further studies are required to depict the role of this area under threatening situations [91], [92], [95].

Cz channel is near the primary motor cortex, located within the precentral gyrus, which controls voluntary motor movements and is responsible for initiating, executing, and coordinating motor actions. The activation of this region may relate to the short movement related to an escape reaction when threat stimulus appears. This is because, when the stimulus suddenly appears towards the participants, they react with a short movement of avoidance, that is, they have a defensive reaction to the threat [91], [92], [95], [96]. This area was also activated with the sound stimulus and in the same frequency band (Table 4). However, a possible explanation for the activation of this area also during the sound stimulus may relate to the fact that the unpredictability of that sound stimulus can also result in a defensive reaction. In fact, some participants also mentioned feeling a little frightened when this auditory stimulus appeared, which may have resulted in the activation of this area to initiate a defensive response (even if that response was not executed).

C3 channel is near the left primary somatosensory cortex, located in the postcentral gyrus, which is responsible for receiving and processing sensory information, such as touch, pressure, temperature and pain. Despite the activation of this area in response to the threat stimulus having no apparent relevance, past studies have also found activity in the left somatosensory cortex in response to fear stimuli not consciously perceived, which could also explain its activation in response to the threat in this study [78], [91], [97], [98].

T3 channel is near the left middle temporal gyrus and left posterior superior temporal gyrus

that have been related to sound recognition, semantic retrieval, processing of mental and verbal arithmetic, and phonological processing for both speech perception and production. Given its sound recognition function, the activation of this area may be related to the sound that accompanies the threat stimulus. However, when only the sound stimulus was presented no activation of this area was observed, so its involvement must be further explored [91], [92], [99].

F8 channel is located near the right inferior frontal gyrus [91]. This area plays a role in attentional processing, being a part of the ventral attentional network responsible for reorienting attention toward salient unexpected stimuli [100], [101]. It is also involved in both implicit and explicit fear processing [17]. In previous studies, the inferior frontal gyrus was found to be involved in sustained fear regulation during an unexpected threat [102], and in anxiety regulation during threat exposure [103]. Thus, given the exposure to an unexpected threat in this study, the activation of this area makes sense. There is also evidence of the involvement of the inferior frontal gyrus in auditory processing [101]. The involvement of the inferior frontal gyrus on diverse brain functions, may be the reason for its activation under the three stimulus conditions (threat, sound and bird).

Fz is located near the premotor and supplementary motor cortex. The functions of the premotor cortex have been related to autonomic reactions and motor responses linked to defensive behaviors [104]. Previous research also found the activation of this area when threatening stimuli enters the peripersonal space [2]. On the other hand, the supplementary motor cortex is involved in the planning and initiation of voluntary motor movement [91], [95], [105], [106]. Thus, these functions have a direct link to the defensive behavior which occurs in response to the exposure to the threatening stimulus of this study.

F7 channel is located near the left inferior frontal gyrus. It has been observed that this area is involved in action preparation and plays a role in threat processing, specifically where the threat is directed towards the person, which represents a direct relation with the threat situation presented in this study (rock that unexpectedly comes toward the participant) [1], [3], [91], [92], [95].

Finally, Fp2 and Fp1 channels are located near the right and left anterior prefrontal cortex,

respectively. The anterior prefrontal cortex is involved in memory retrieval and executive function such as reasoning, planning, execution, decision making and processing emotional stimuli. Given the complexity of the prefrontal cortex functions, there are a wide range of mechanisms that can lead to its activation under threat stimulus. For instance, this area is shown to be involved in the control of fear behavior, and composes the amygdala-dorsomedial prefrontal circuit which has been shown to be involved in threat vigilance, once it's responsible to promote attention to threat, and in the regulation of responses to salient stimuli (including cues of threat). Moreover, given the proximity of these electrodes to the forehead and the eyes, one cannot rule out the hypothesis that the activation of these electrodes could be due to eye movements and blinking or, also, to muscular artifacts associated with the forehead muscles, which could have not been completely removed in the preprocessing phase [3], [91], [92], [95], [107], [108].

The goal of obtaining the brain areas and frequency bands activated for each of the 3 different stimuli (threat, sound and bird) was to posteriorly discard activations associated with other phenomena than the threat situation. Comparing the threat stimulus results with the sound stimulus results (Table 4), the activations found in common were Cz-beta, F8-beta, and F8-delta. This way, F8-beta and F8-delta won't be considered relevant for the threat situation. Regarding Cz-beta, as mentioned before, Cz activation is possibly related to the defensive motor activity resulting from the sudden and unexpected appearance of these two stimuli, so the relevance of the beta band of this channel for the threat situation won't be discarded. Comparing the threat stimulus results with the bird stimulus results (Table 4), the only activation found in common was F8-beta, which was also found for the sound stimulus. So, as mentioned before, F8-beta will not be considered relevant for the threat situation.

Finally, regarding the threatening stimulus, in Table 4 it is possible to observe the predominance of the delta, beta and gamma bands, appearing as significant in several channels, and the absence of the theta band. The alpha band is also almost non-existent, manifesting in only one channel. The relevance of these frequency bands should be analyzed in more detail in further studies. However, it should be noted that, in relation to the delta and gamma bands specifically, there is always the hypothesis that their predominance may not necessarily be

linked to threat processing but rather to the permanence of EEG artifacts that were not completely removed in the preprocessing phase. This is because eye blinking and eye movement artifacts contain frequencies belonging to the delta band, and muscle activity artifacts are related to higher frequencies that fall in the gamma band. Therefore, the analysis of the relevance and involvement of these frequency bands in threat processing must be cautious.

5.2.2. Overall Discussion

After this comparison analysis, another analysis was performed. As mentioned in section 4.3.2, along the experimental phase, twenty participants reacted to the threat stimulus, while six did not (and they were excluded from the previous analysis). Therefore, to corroborate the relevant brain areas obtained for the threatening situation, the same analysis was performed using only these six participants. Interestingly, no significant differences were obtained between the neutral and threat stimulus states for any of the brain areas. Despite the reduced number of participants included in this second analysis (only six), and the consequent statistical limitations, it was previously observed that, when also analyzing a reduced number of participants that felt threatened (a subset of the twenty participants), significant differences were observed and agreed with those obtained for the twenty participants. This indicates that the lack of significant differences for the case of the six participants who did not feel threatened by the threat stimulus was not a consequence of the analysis including a reduced number of data, but rather an indicator that those who did not feel threatened by the stimulus most likely did not activate brain areas in response to the stimulus. This way, this analysis evidences the consistency of our results and observations.

Finally, Figure 21 represents the relevant channels and frequency bands under threat stimulus, found in the aforementioned analysis. Globally, it is possible to observe that most discriminative brain regions between the neutral and threat states are located in the front half of the brain and slightly more concentrated in the left hemisphere.

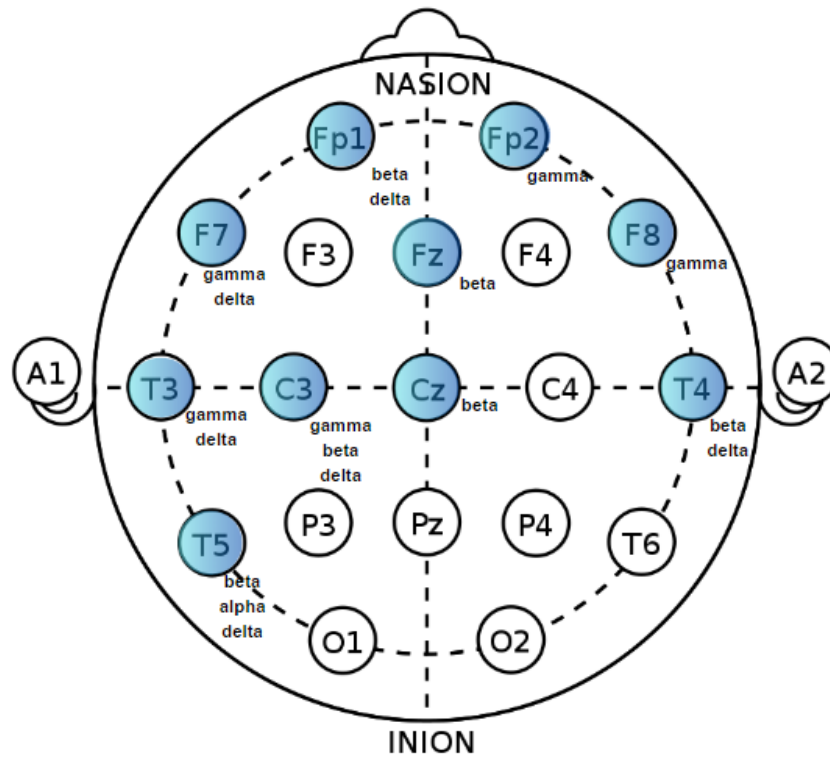


Figure 21: Relevant channels and frequency bands in the threat stimulus situation. Relevant channels are marked in blue.

In general, these results are consistent with the literature, as there are many areas found in common with the other threat processing studies carried out so far. The obtained common areas are: the inferior frontal gyrus, premotor cortex, supplementary motor cortex, prefrontal cortex, superior temporal gyrus and middle temporal gyrus [1]–[3].

More specifically, this study focuses on the defensive reaction to a threat situation. And, in fact, motor areas responsible for motor actions that may relate to the short movement linked to an escape reaction, were activated in response to the threat stimulus.

Moreover, given its role in visual perception, which concerns the ability to receive, interpret and react to visual stimuli, at first sight, one would expect the existence of significant differences between the visual threatening stimulus and neutral states for the primary visual

cortex (O1 and O2 channels). However, the lack of significant differences associated with this area may be because, even in the neutral parts of the video, there are many visual elements appearing in the scene such as trees, flowers and grass. On the other hand, the absence of significant differences between the neutral and threat stimulus for the visual cortex but the found significance of the motor areas, could reflect that, when considering a fast unexpected visual threat, a defensive reaction can be originated even in the absence of visual stimuli processing and recognition by the visual cortex. This could mean that, in a situation of unconscious processing of a visual-related threat, it takes place an unconscious processing that bypasses the visual cortex and, that way, enables a rapid and automatic defensive response to the threat, as reported in past studies [77], [78].

In addition, the amygdala also seems to be linked to perception of threat and danger, once it is one of the brain regions most found in threat processing research (section 3.2). However, the amygdala is a deep structure of the brain, and so EEG, the brain recording technique used in this study, cannot measure its activity.

5.3. Functional Connectivity Between Relevant Brain Areas

5.3.1. COH, iCOH, wPLI and MPC Results

In Figures 22 to 25 are shown, for the COH, iCOH, wPLI, and MPC methods, the matrices containing the connectivity values of each pair of channels and for each condition: neutral state (pre-stimulus), threat stimulus state (post-stimulus) and the difference between the connectivity values of the stimulus and neutral states (pos-pre), as well as the resulting brain diagram containing the connections whose differences between the connectivity values of the stimulus and neutral states are higher than a threshold, indicating the relevance of these connections. The threshold value corresponds to the 0.65-quantile, that is, it corresponds to the connectivity value above which 35% of the highest connectivity values are.

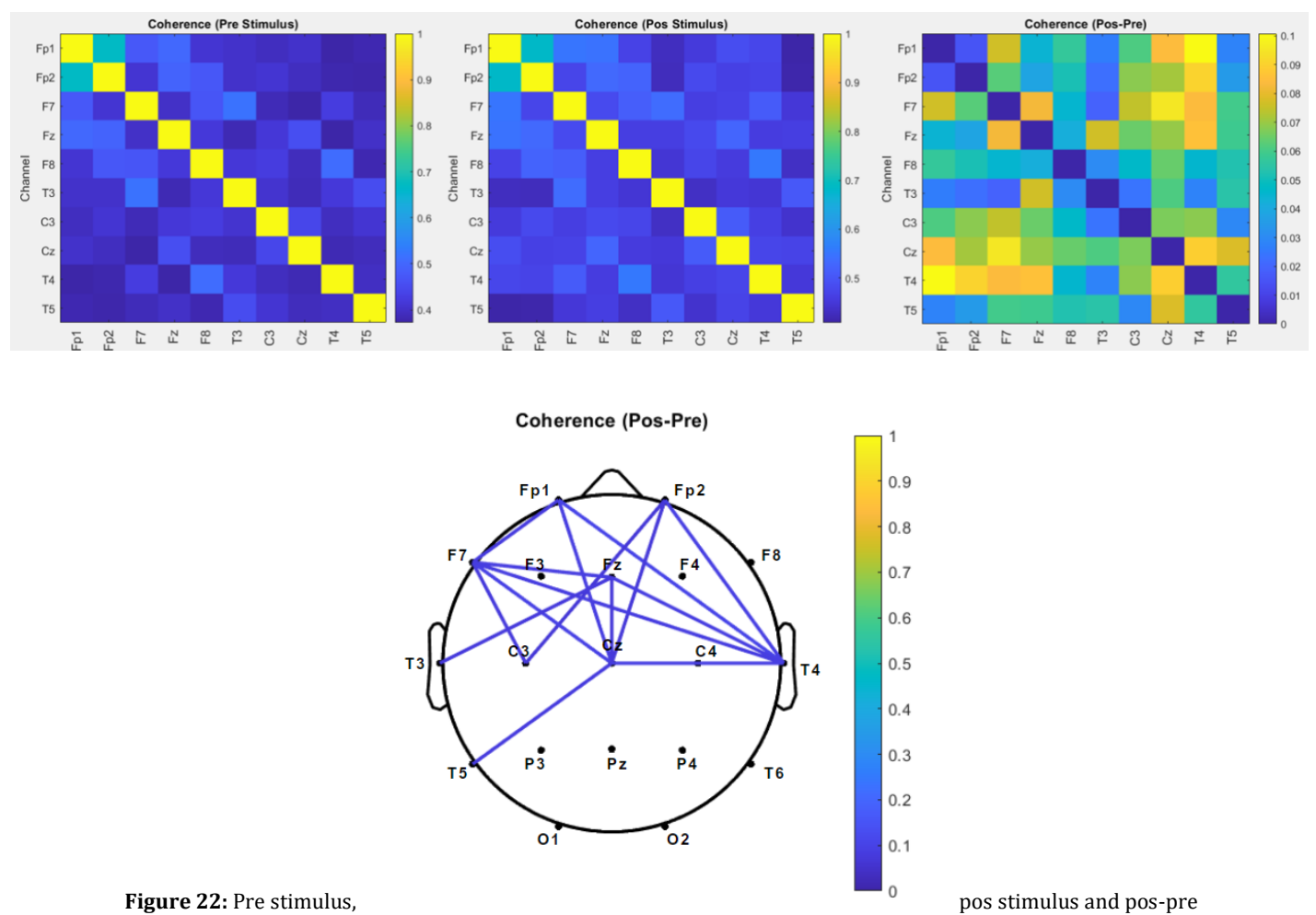
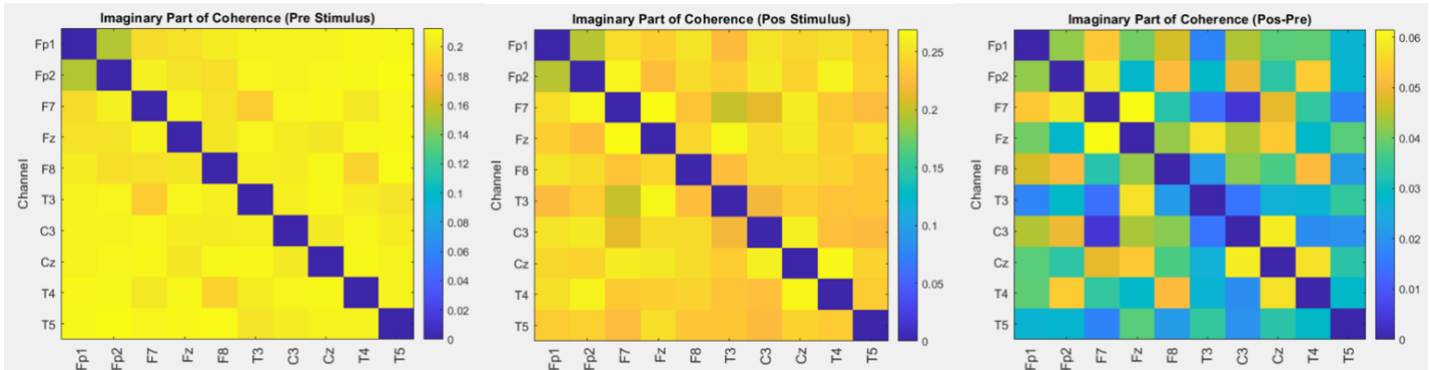


Figure 22: Pre stimulus, pos stimulus and pos-pre stimulus COH matrices and pos-pre stimulus brain connectivity representation.



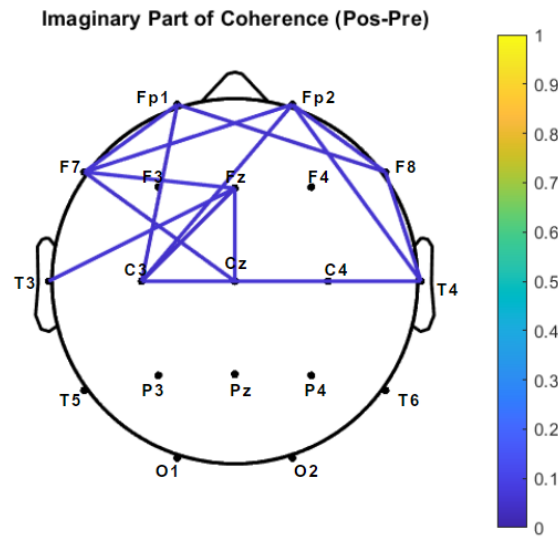


Figure 23: Pre stimulus, pos stimulus and pos-pre stimulus iCOH matrices and pos-pre stimulus brain connectivity representation.

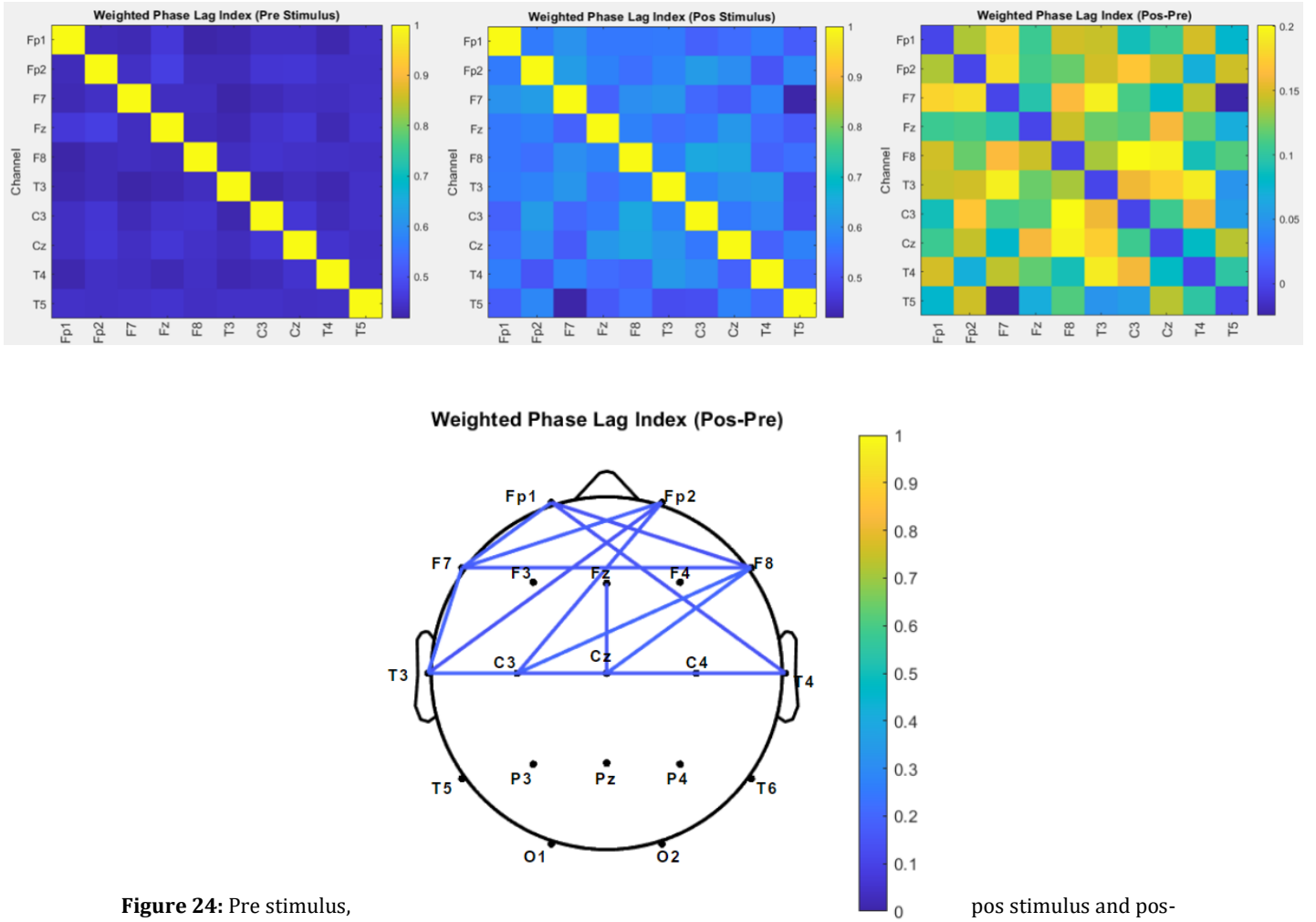
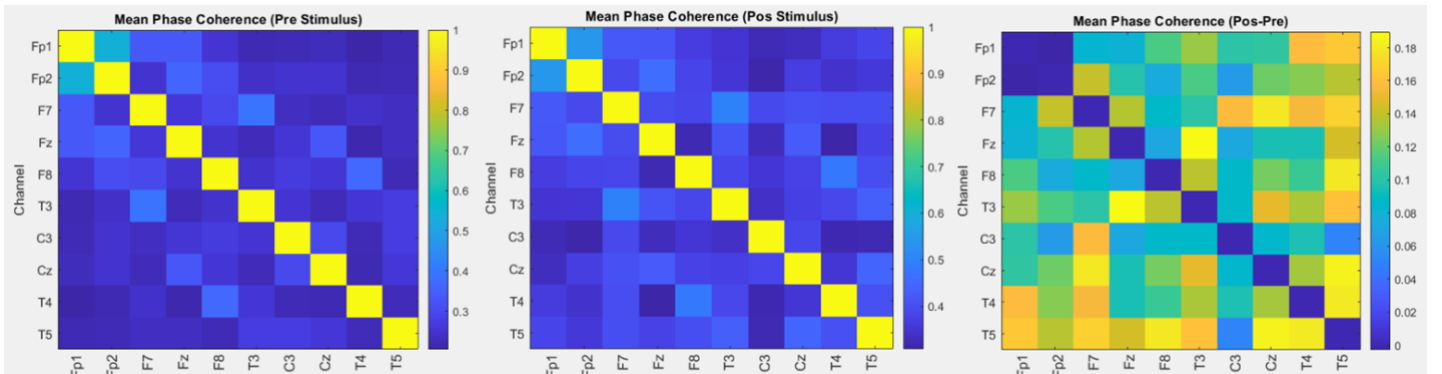
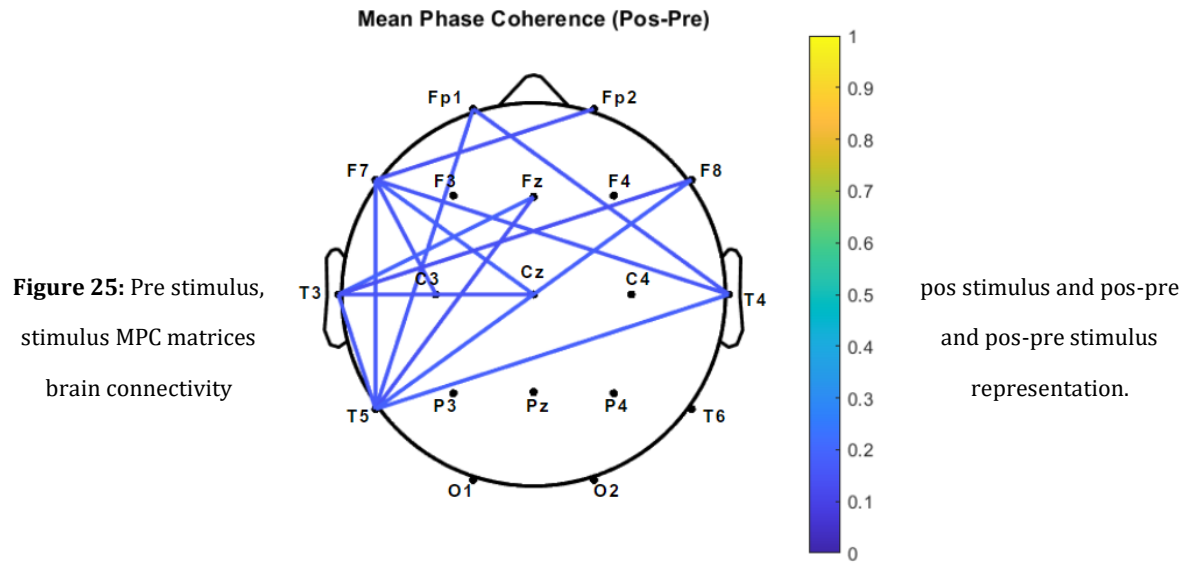


Figure 24: Pre stimulus, pos stimulus and pos-pre stimulus wPLI matrices and pos-pre stimulus brain connectivity representation.





Following calculation of the connectivity values, the Kruskal-Wallis test with a significance level of 5% and a posterior multiple comparison correction (Holm-Bonferroni and FDR) was performed. The obtained significant connections of each method are present in Table 5.

Table 5: Channel connections that presented significant differences between the neutral state and the threat stimulus state for each of the connectivity methods, using a significance level of 0.05, and after the multiple comparison correction.

Correction Method	COH	iCOH	wPLI	MPC
-------------------	-----	------	------	-----

Holm-Bonferroni	F7-Cz	Fz-T3 Fz-Cz	–	F7-C3
FDR	–	Fz-T3 Fz-Cz	–	–

Table 6 shows the significant connections obtained after the performance of the posterior Kruskal-Wallis test with a significance level of 1% and without multiple comparison correction, for each of the connectivity methods.

Table 6: Channel connections that presented significant differences between the neutral state and the threat stimulus state for each of the connectivity methods, using a significance level of 0.01, without multiple comparison correction.

Connections	COH	iCOH	wPLI	MPC
Fp1-T4	▪			
Fp1-C3				▪
Fp1-T5				▪
Fp2-F7				▪
Fp2-T4	▪	▪		
F7-Cz	▪			▪
F7-T4	▪		▪	
F7-F8			▪	
F7-T3			▪	
F7-C3				▪
Fz-T3	▪	▪		
Fz-F8		▪		
Fz-Cz		▪		
F8-C3			▪	

Cz-T5	▪	▪		▪
T3-Cz			▪	
T3-T4			▪	

Finally, Table 7 shows the connections that presented values of the difference between the connectivity values of the threat stimulus and neutral states (pos-pre) higher than the 0.65-quantile, for each of the connectivity methods. To obtain more reliable results, only the connections presented in Table 7 that are present in at least three of the connectivity methods were considered relevant. Table 7 includes the channel pairs and the correspondent difference values for each method, as well as the connections in common with at least three of the methods (in the last column).

Table 7: Channel connections presenting differences between the connectivity values of the threat stimulus and neutral states (pos-pre) higher than the 0.65-quantile for each of the connectivity methods, and connections in common with at least three of the methods (in the last column). The values in bold represent the connections with the highest Pos-Pre connectivity values of each method.

Connections	COH	iCOH	wPLI	MPC	Common
Fp1-T4	0.100		0.147	0.158	▪
Fp1-Cz	0.084				
Fp1-F7	0.076	0.053	0.178		▪
Fp1-F8		0.046	0.146		
Fp1-C3		0.044			
Fp1-T5				0.164	
Fp2-Cz	0.070				
Fp2-C3	0.068	0.049	0.170		▪
Fp2-F7		0.058	0.184	0.140	▪
Fp2-F8		0.051			

Fp2-T3			0.147		
Fp2-T4	0.090	0.054			
F7-Cz	0.095	0.048		0.179	▪
F7-T4	0.084			0.155	
F7-Fz	0.082	0.061			
F7-C3	0.074			0.157	
F7-T3			0.194		
F7-F8			0.163		
F7-T5				0.169	
Cz-T4	0.089	0.057			
Cz-T5	0.078			0.184	
Fz-T4	0.085				
Fz-T3	0.076	0.057		0.189	▪
Fz-Cz	0.069	0.053	0.160		▪
Fz-C3		0.043			
Fz-T5				0.144	
C3-Cz		0.059			
C3-T4			0.160		
F8-T4		0.051			
F8-C3			0.200		
F8-Cz			0.195		
F8-T5				0.179	
F8-T3				0.138	
T3-T4			0.191		
T3-Cz			0.175	0.150	
T3-C3			0.158		
T3-T5				0.160	
T4-T5				0.181	

5.3.2. Discussion

Analyzing the difference matrix (Pos-Pre) obtained for the COH method (Figure 22), it is observed that the channel connections that present the highest difference between the connectivity values of the two conditions are: Fp1-T4, F7-Cz, Fp2-T4, Cz-T4, Fz-T4, Fp1-Cz and F7-T4, with differences in the connectivity values of 0.100, 0.095, 0.090, 0.089, 0.085, 0.084331 and 0.084007, respectively. Regarding the difference matrix (Pos-Pre) of the iCOH method (Figure 23), it is observed that the channel connections that present the highest difference values between the connectivity values of the two conditions are: F7-Fz, C3-Cz, Fp2-F7, Fz-T3 and Cz-T4, with differences in the connectivity values of 0.061, 0.059, 0.058, 0.057 and 0.057, respectively. Analyzing the difference matrix (Pos-Pre) of wPLI (Figure 24), it is observed that the channel connections that present the highest differences in the connectivity values of the two conditions are: F8-C3, F8-Cz, F7-T3, T3-T4 and Fp2-F7, with difference connectivity values of 0.200, 0.195, 0.194, 0.191 and 0.184, respectively. Finally, analyzing the MPC difference matrix (Pos-Pre) (Figure 25), it is observed that the channel connections that present the highest differences in the connectivity values of the two conditions are: Fz-T3, Cz-T5, T4-T5, F7-Cz and F8-T5, with difference connectivity values of 0.189, 0.184, 0.181, 0.179 and 0.179, respectively.

Comparing the list of relevant connections common to at least three of the four methods (Table 7) with the connections with the highest Pos-Pre connectivity values (mentioned above) of each method, four pairs of connected areas are found in common: Fp1-T4, Fp2-F7, Fz-T3 and F7-Cz. The connections with the highest Pos-Pre connectivity values of each method are highlighted in bold in Table 7.

Regarding the results of the Kruskal-Wallis test with a significance level of 5% and a posterior multiple comparison correction (Table 5), it's possible to observe that few significant connections were found for each method, and no coincident connections were found between methods. On the other hand, the Kruskal-Wallis test with a smaller significance level of 1% and without multiple comparison correction (Table 6) resulted in a slightly larger number of significant connections for each method, but only one connection was common to at least three of the four methods. Finally, the new approach (using the matrix of the Pos-Pre values

combined with a defined threshold, instead of a statistical test) provided better results, once seven relevant connections common to at least three of the connectivity methods were found (Table 7). These results presented in Table 7 will be explored in more detail in section 5.4.

5.4. Threat Brain Network

5.4.1. Results

From the analyses carried out in the previous step, it is concluded that the most consistent observations related to the threat situation are the connectivity in Fp1-F7, Fp1-T4, Fp2-F7, Fp2-C3, Fz-T3, F7-Cz and Fz-Cz, as shown in Table 7. Therefore, these will be the connections considered relevant in this study. Figure 26 represents these connections as well as their directions (represented by arrows) which were obtained by analyzing the $DTF(i,j)$ and $DTF(j,i)$ values of the corresponding channel pairs.

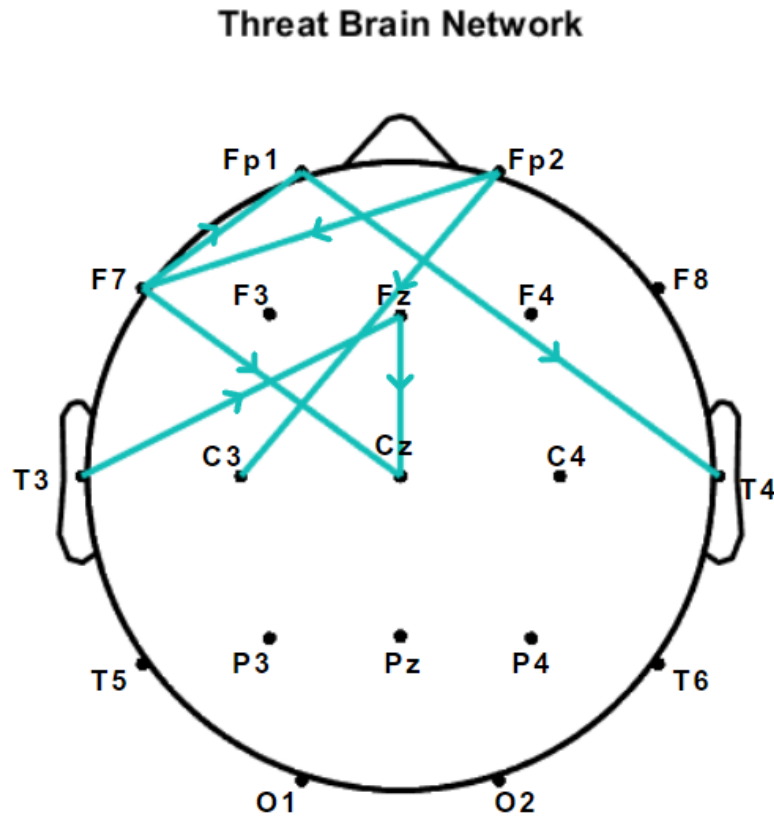


Figure 26: Schematic representation of the brain connectivity and directionality (represented by arrows) found for the threat situation.

5.4.2. Discussion

Observing Figure 26, it is possible to identify that all the significant connections are concentrated in the front half of the brain and slightly more concentrated in the left hemisphere.

Once the goal is to study the neural correlates behind the defensive response after exposure to an unexpected threat, it is important to analyze the connections involving the motor areas. The motor areas are responsible for initiation and execution of motor movements and so are expectable to be involved in defensive behaviors. The motor areas obtained as significant here are the ones associated with Cz and Fz channels. From Figure 26, it is observed that the

connections involving these motor areas represent an influx of information directed to them. It is observed a connection from the F7 channel to the Cz channel. F7 englobes a region (left inferior frontal gyrus) that has been shown to play a role in threat processing, specifically where the threat is directed towards the person [1], [3]. This could mean that, when a threat is coming towards a person, there's an activation of the left inferior frontal gyrus which in turn activates the Cz motor area to produce a motor defensive response. It is also observed a connection from the T3 channel to the Fz channel. Since the regions located near the T3 channel present functions mainly associated with sound processing [92], [99], this connection doesn't seem to be relevant at first sight. Thus, this connection should be studied and explained in further studies with different techniques to better infer its relevance and meaning. Still regarding the motor areas, there is also a connection between them, directed from Fz to Cz. It is known that the premotor cortex (located close to the Fz channel) influences motor responses through reciprocal connections with the primary motor cortex (located close to the Cz channel), which may explain the observed Fz-Cz connectivity [109].

Since the threatening stimulus concerns the appearance of an unexpected visual threat, other important connections to be analyzed would be those involving the visual cortex, more specifically the influx of information from this area to others. This is because the visual cortex is responsible for receiving, integrating and processing visual information that arrives from the retina. However, this area is located in the occipital lobe, corresponding to the O1 and O2 channels, and, for these channels, there were not found significant differences between the neutral and threat states (section 5.2.1). Therefore the connectivity analysis did not include these channels, once they were not considered relevant due to the lack of significant differences. However, as already mentioned, this lack of significant differences associated with the visual cortex may relate to the existence of an unconscious processing network that bypasses this area and enables a rapid defensive response induced by threats.

The remaining connections involving the prefrontal cortex (F7-Fp1, Fp1-T4, Fp2-F7 and Fp2-C3), are not surprising because of the known functions of this brain region in guiding actions, thoughts and emotions [92], [95]. However, additional studies involving other techniques are needed to gain more insights into the functional connectivity of this area under

threat stimulus.

It should be noted that we restricted the analysis to connections found by at least three of the four applied connectivity methods to increase the reliability of the observations. However, and due to this restriction, it is quite likely that there are other meaningful connections induced by the threat stimulus that were not discussed.

5.5. Frequency Bands Connectivity Analysis

5.5.1. Results

Figure 27 presents the COH matrices obtained for the difference between the COH values of the threat stimulus and neutral states (post-pre), for each frequency band: delta, theta, alpha, beta and gamma.

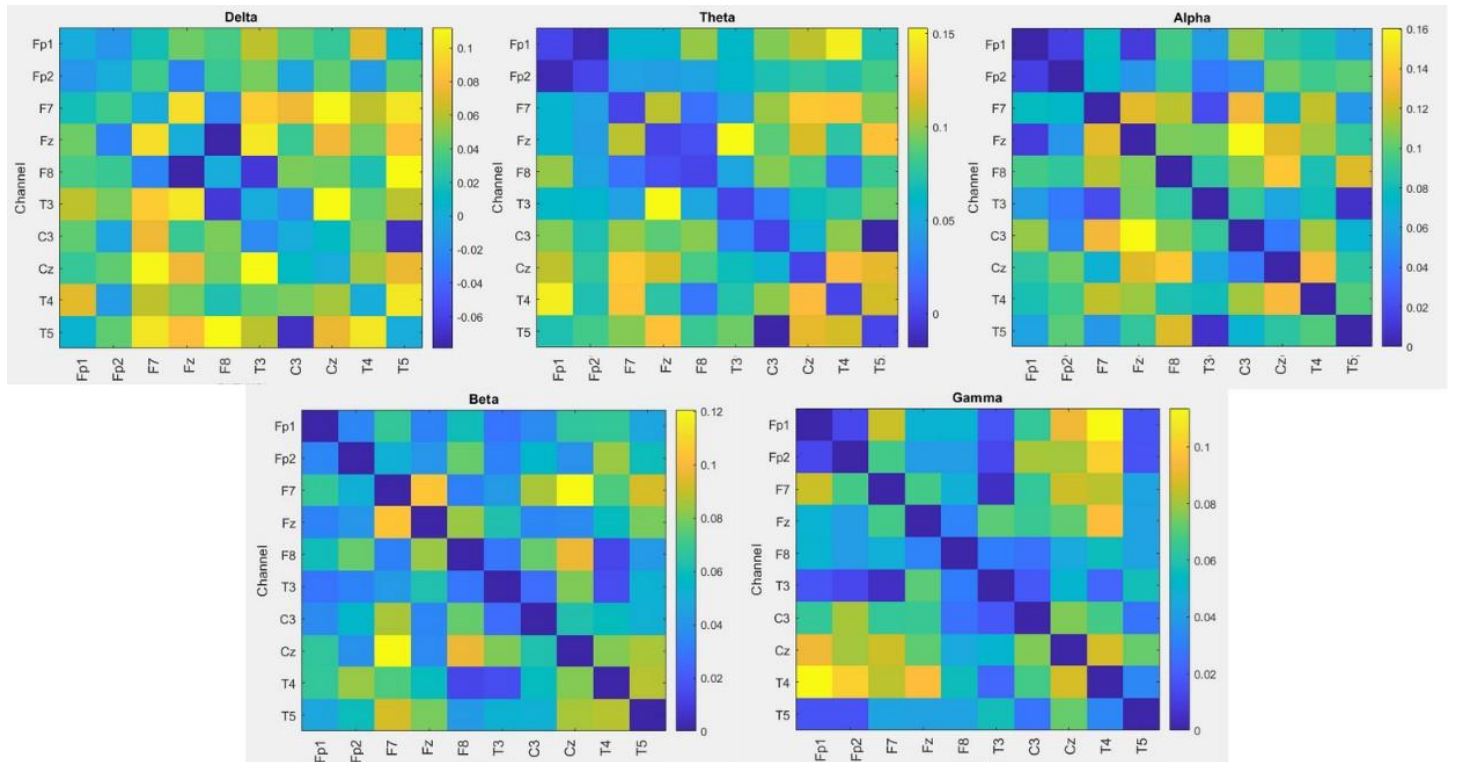


Figure 27: COH matrices for all the frequency bands.

5.5.2. Discussion

Observing Figure 27, different connectivity patterns are found for different frequency bands, and a detailed discussion about these differences will not be addressed in this report. However, at first sight, it is possible to observe that there is no frequency band that stands out particularly from the others for having higher difference values between the neutral and threat conditions, once for all the frequency bands, the highest COH difference values are very similar (all around 0.15).

However, it should be noted that this analysis studies the connectivity between brain areas in the same frequency band, and two areas can actually be connected in different frequency bands. That is, brain areas x and y can actually be connected, but instead of both being connected in frequency band 1, area x can be in frequency band 1 and area y in frequency band 2, for example. Therefore, further studies should analyze this hypothesis.

6. Acquired Competencies

Throughout the course of this thesis project, a diverse range of competencies of distinct nature have been acquired. This is because this project involved many steps and tasks in diverse fields, namely VR development, EEG acquisitions, data preprocessing and functional connectivity analysis. These acquired competencies have been instrumental in the execution of the project and have significantly contributed to expanding knowledge and acquiring skills in these areas.

One of the main skills acquired concerns VR management and the development of VR videos. This was an area that was learned from scratch as it had never been explored prior to the development of this project and therefore the knowledge was very limited. Although it is a complex area, through dedicated research and practical implementation, the principles and techniques involved in creating immersive virtual reality experiences were learned and knowledge about VR software tools and platforms was also successfully acquired. More specifically, the VR platform used in the development of this project, Unity, provided useful and easy-to-learn tools to develop VR videos. This hands-on experience provided the necessary skills to conceptualize, design and implement VR video content effectively.

As a significant component of the project, EEG acquisitions were also performed from scratch. After familiarization with the theoretical foundations of EEG measurements, electrode placement and best practices for data acquisition, through meticulous experimentation and previous tests, practical expertise was developed in setting up EEG recording sessions, calibrating the equipment, and ensuring optimal signal quality. Before acquiring the data of the 26 participants and, since the EEG acquisitions were going to be performed without supervision, many previous acquisitions were made with the aim of understanding the whole process as much as possible and, that way, optimizing the quality of the data collection. This allowed a reliable and accurate acquisition of EEG signals for subsequent analysis.

In addition, despite being an area more worked on in past projects and, therefore, in which some knowledge prior to this project already existed, data processing was also a competence

that was further developed with the aid of relevant literature. Thereby, proficiency was gained in pre-processing raw EEG data, including artifact removal, filtering, and extraction of relevant features.

By employing functional connectivity methods such as coherence, imaginary part of coherence, weighted phase lag index, mean phase coherence and directed transfer function, insights into the complex network dynamics and relationships between brain regions were gained, as well as knowledge in implementing functional connectivity methods.

Concluding, these acquired competencies have been pivotal in conducting a comprehensive investigation into the impact of threatening situations on brain activation and brain connections involved. Also, the newfound expertise in VR development and EEG data acquisition has allowed to gain competencies in completely new areas.

7. Conclusion

The goal of this study consisted of finding the brain areas activated in response to an unexpected visual threat, and the connectivity between those areas. With this purpose, a threat scene was created by VR, and the brain activity of twenty-six participants was recorded using a 19 channel EEG, while viewing the threat scene with a VR headset.

The brain areas activated by the applied threat stimulus consisted of the associative visual cortex, superior and middle temporal gyrus, primary motor cortex, primary somatosensory cortex, premotor and supplementary motor cortex, inferior frontal gyrus and anterior prefrontal cortex. Most of these areas are consistent with the ones found in the literature [1]–[3]. The involvement of these areas in unexpected visual threat situations may be related to their known role in visual information processing (left associative visual cortex), sustained fear regulation and anxiety regulation during an unexpected threat (right inferior frontal gyrus), reorienting attention toward salient unexpected stimuli (right inferior frontal gyrus), promoting attention to threat (prefrontal cortex) and planning and execution of avoidance strategies and defensive behaviors (primary motor cortex, and premotor and supplementary motor cortex). Additionally, the lack of the visual cortex activation but the observed activation of the motor areas, could reflect that, when considering a fast unexpected visual threat, a defensive reaction can be originated even in the absence of visual stimuli processing and recognition by the visual cortex. This could mean that, in a situation of unconscious processing of a visual threat, it takes place a process that bypasses the visual cortex, and enables a rapid and automatic defensive response. The results also show the relevance of delta, beta and gamma frequency bands in threat processing.

The functional connectivity analysis was performed recurring to the COH, iCOH, wPLI, MPC and DTF methods, obtaining diverse relevant connections related to the threat situation and in common with almost all of the methods, as: Fp1-F7, Fp1-T4, Fp2-F7, Fp2-C3, Fz-T3, F7-Cz and Fz-Cz. These connections are concentrated in the front half of the brain and slightly more concentrated in the left hemisphere. There is an influx of information from the left inferior

frontal gyrus (F7 channel) and left middle temporal gyrus (T3 channel) to the motor areas primary motor cortex (Cz channel) and premotor cortex (Fz channel). The left inferior frontal gyrus is involved in threat processing especially when the threat is directed towards the person, which could mean that, when a threat is coming towards a person, there's an activation of this area which in turn activates the primary motor cortex to produce a motor defensive response. It was also found an influx of information from the premotor cortex to the primary motor cortex, which could mean that these areas work together to originate a defensive response. The remaining found connections (F7-Fp1, Fp1-T4, Fp2-F7 and Fp2-C3) involve the prefrontal cortex, which is not surprising due to the known functions of this brain region in guiding actions, thoughts and emotions.

Regarding the frequency-specific connectivity analysis, different Pos-Pre connectivity patterns were found for the different frequency bands. Globally, it is observed that there is no frequency band that stands out particularly from the others for having higher Pos-Pre connectivity values. However, since this analysis studies the connectivity between brain areas in the same frequency band, this may indicate that two areas can actually be connected in different frequency bands. This way, performing a future cross-frequency connectivity analysis, could lead to additional information and additional relevant results.

One inherent limitation in EEG studies is the spatial resolution. This way, and once the EEG cap used in this study is composed of only 19 electrodes, in future works, using an EEG cap with a higher number of electrodes could provide a better spatial coverage and allow the detection of more subtle brain dynamics possibly relevant for the study of the brain during threat. Another future step for this study would be to find the temporal sequence of activation of the different relevant brain areas.

As a final note, it is concluded that the objective of this project was achieved, since it was possible to discover the relevant brain areas involved in response to threatening stimulus, and also the significant connections between them and the consequent neuronal network. These results contribute to the understanding of defensive reactions that may, in the future, support the development of treatments for certain pathological conditions. Additionally, throughout the course of this project, a range of new and important skills of distinct nature were acquired,

especially related to VR, signal acquisition and processing domains, that may serve for the development of future research. Ultimately, the EEG data acquired in this study allowed the creation of a new database that can serve as a basis for future research in this field.

References

- [1] S. Pichon, B. de Gelder, and J. Grèzes, "Threat prompts defensive brain responses independently of attentional control," *Cereb. Cortex N. Y. N* 1991, vol. 22, no. 2, pp. 274–285, Feb. 2012, doi: 10.1093/cercor/bhr060.
- [2] A. W. de Borst and B. de Gelder, "Threat Detection in Nearby Space Mobilizes Human Ventral Premotor Cortex, Intraparietal Sulcus, and Amygdala," *Brain Sci.*, vol. 12, no. 3, p. 391, Mar. 2022, doi: 10.3390/brainsci12030391.
- [3] O. Fernandes *et al.*, "How do you perceive threat? It's all in your pattern of brain activity," *Brain Imaging Behav.*, vol. 14, no. 6, pp. 2251–2266, Dec. 2020, doi: 10.1007/s11682-019-00177-6.
- [4] E. Vagnoni, S. F. Lourenco, and M. R. Longo, "Threat modulates neural responses to looming visual stimuli," *Eur. J. Neurosci.*, vol. 42, no. 5, pp. 2190–2202, Sep. 2015, doi: 10.1111/ejn.12998.
- [5] M. Yilmaz Balban *et al.*, "Human Responses to Visually Evoked Threat," *Curr. Biol. CB*, vol. 31, no. 3, pp. 601–612.e3, Feb. 2021, doi: 10.1016/j.cub.2020.11.035.
- [6] A. E. Gümüş, C. Uyulan, and Z. Guleken, "Detection of EEG Patterns for Induced Fear Emotion State via EMOTIV EEG Testbench," *Nat. Eng. Sci.*, vol. 7, pp. 148–168, Aug. 2022, doi: 10.28978/nesciences.1159248.
- [7] J. C. Cléry *et al.*, "Looming and receding visual networks in awake marmosets investigated with fMRI," *NeuroImage*, vol. 215, p. 116815, Jul. 2020, doi: 10.1016/j.neuroimage.2020.116815.
- [8] G. H. Glover, "Overview of Functional Magnetic Resonance Imaging," *Neurosurg. Clin. N. Am.*, vol. 22, no. 2, pp. 133–139, Apr. 2011, doi: 10.1016/j.nec.2010.11.001.
- [9] K. A. Maldonado and K. Alsayouri, "Physiology, Brain," in *StatPearls*, Treasure Island (FL): StatPearls Publishing, 2023. Accessed: Oct. 25, 2022. [Online]. Available: <http://www.ncbi.nlm.nih.gov/books/NBK551718/>
- [10] "Figure 2.1: The different regions and parts of the human brain. The...", *ResearchGate*. https://www.researchgate.net/figure/The-different-regions-and-parts-of-the-human-brain-The-cortex-is-located-at-the_fig1_318507477 (accessed Jan. 25, 2023).
- [11] M. F. Bear, B. W. Connors, and M. A. Paradiso, *Neuroscience: Exploring the brain*, 3rd ed. in *Neuroscience: Exploring the brain*, 3rd ed. Philadelphia, PA, US: Lippincott Williams & Wilkins Publishers, 2007, pp. xxxviii, 857.
- [12] "Visual Pathway & Visual Field Defects | Lecturio Medical." <https://www.lecturio.com/concepts/the-visual-pathway-and-related-disorders/> (accessed Jan. 18, 2023).
- [13] "Persistent fear responses in rhesus monkeys to the optical stimulus of 'looming' - PubMed." <https://pubmed.ncbi.nlm.nih.gov/14498362/> (accessed Jul. 31, 2023).
- [14] F. R. R. van der Weel and A. L. H. van der Meer, "Seeing it coming: infants' brain responses to looming danger," *Naturwissenschaften*, vol. 96, no. 12, pp. 1385–1391, Dec. 2009, doi: 10.1007/s00114-009-0585-y.
- [15] J. Billington, R. M. Wilkie, D. T. Field, and J. P. Wann, "Neural processing of imminent collision in humans," *Proc. Biol. Sci.*, vol. 278, no. 1711, pp. 1476–1481, May 2011, doi: 10.1098/rspb.2010.1895.
- [16] C. Bertini and E. Làdavas, "Fear-related signals are prioritised in visual, somatosensory and spatial systems," *Neuropsychologia*, vol. 150, p. 107698, Jan. 2021, doi: 10.1016/j.neuropsychologia.2020.107698.
- [17] D. Tao, Z. He, Y. Lin, C. Liu, and Q. Tao, "Where does fear originate in the brain? A coordinate-based meta-analysis of explicit and implicit fear processing," *NeuroImage*, vol. 227, p. 117686, Feb. 2021,

- doi: 10.1016/j.neuroimage.2020.117686.
- [18] P. Sah, "Fear, Anxiety, and the Amygdala," *Neuron*, vol. 96, no. 1, pp. 1–2, Sep. 2017, doi: 10.1016/j.neuron.2017.09.013.
- [19] L. Pessoa and R. Adolphs, "Emotion processing and the amygdala: from a 'low road' to 'many roads' of evaluating biological significance," *Nat. Rev. Neurosci.*, vol. 11, no. 11, pp. 773–783, Nov. 2010, doi: 10.1038/nrn2920.
- [20] Y. Litvin, D. C. Blanchard, and R. J. Blanchard, "Chapter 5.1 - Vocalization as a social signal in defensive behavior," in *Handbook of Behavioral Neuroscience*, S. M. Brudzynski, Ed., in *Handbook of Mammalian Vocalization*, vol. 19. Elsevier, 2010, pp. 151–157. doi: 10.1016/B978-0-12-374593-4.00015-2.
- [21] D. C. Blanchard, E. B. Defensor, and R. J. Blanchard, "Fear, Anxiety, and Defensive Behaviors in Animals," in *Encyclopedia of Behavioral Neuroscience*, G. F. Koob, M. L. Moal, and R. F. Thompson, Eds., Oxford: Academic Press, 2010, pp. 532–537. doi: 10.1016/B978-0-08-045396-5.00090-7.
- [22] F. Rigoli, M. Ewbank, T. Dalgleish, and A. Calder, "Threat visibility modulates the defensive brain circuit underlying fear and anxiety," *Neurosci. Lett.*, vol. 612, pp. 7–13, Jan. 2016, doi: 10.1016/j.neulet.2015.11.026.
- [23] K. Amano, N. Goda, S. Nishida, Y. Ejima, T. Takeda, and Y. Ohtani, "Estimation of the timing of human visual perception from magnetoencephalography," *J. Neurosci. Off. J. Soc. Neurosci.*, vol. 26, no. 15, pp. 3981–3991, Apr. 2006, doi: 10.1523/JNEUROSCI.4343-05.2006.
- [24] "In the blink of an eye," *MIT News | Massachusetts Institute of Technology*, Jan. 16, 2014. <https://news.mit.edu/2014/in-the-blink-of-an-eye-0116> (accessed Nov. 25, 2022).
- [25] M. C. Potter, B. Wyble, C. E. Hagmann, and E. S. McCourt, "Detecting meaning in RSVP at 13 ms per picture," *Atten. Percept. Psychophys.*, vol. 76, no. 2, pp. 270–279, Feb. 2014, doi: 10.3758/s13414-013-0605-z.
- [26] C. Baiano and M. Zeppieri, "Visual Evoked Potential," in *StatPearls*, Treasure Island (FL): StatPearls Publishing, 2023. Accessed: Aug. 03, 2023. [Online]. Available: <http://www.ncbi.nlm.nih.gov/books/NBK582128/>
- [27] D. J. Creel, "Chapter 34 - Visually evoked potentials," in *Handbook of Clinical Neurology*, K. H. Levin and P. Chauvel, Eds., in *Clinical Neurophysiology: Basis and Technical Aspects*, vol. 160. Elsevier, 2019, pp. 501–522. doi: 10.1016/B978-0-444-64032-1.00034-5.
- [28] Kriso.ee, *Bradley and Daroff's Neurology in Clinical Practice, 2-Volume Set 8th edition - Joseph Jankovic, John C Mazziotta, Scott L ... - 9780323642613 - Book | Kriso.ee*. [Online]. Available: <https://www.kriso.ee/bradley-daroffs-neurology-clinical-practice-2-db-9780323642613.html>
- [29] R. N. F. and M. J. del R., *Brain-Computer Interfaces*. Elsevier, 2020.
- [30] V. S. Ramachandran, *Encyclopedia of Human Behavior: Second edition*. 2012, p. 2518.
- [31] A. Jalilifard, A. Rastegarnia, E. Pizzolato, and Md. K. Islam, "Classification of Emotions Induced by Horror and Relaxing Movies Using Single-Channel EEG Recordings," *Int. J. Electr. Comput. Eng.*, vol. 10, pp. 3826–3838, Feb. 2020, doi: 10.11591/ijece.v10i4.pp3826-3838.
- [32] P. Abhang, B. Gawali, and S. Mehrotra, "Technological Basics of EEG Recording and Operation of Apparatus," 2016, pp. 19–50. doi: 10.1016/B978-0-12-804490-2.00002-6.
- [33] N. Masood and H. Farooq, "Investigating EEG Patterns for Dual-Stimuli Induced Human Fear Emotional State," *Sensors*, vol. 19, no. 3, p. 522, Jan. 2019, doi: 10.3390/s19030522.
- [34] C. S. Nayak and A. C. Anilkumar, "EEG Normal Waveforms," in *StatPearls*, Treasure Island (FL): StatPearls Publishing, 2023. Accessed: Aug. 03, 2023. [Online]. Available: <http://www.ncbi.nlm.nih.gov/books/NBK539805/>
- [35] A. S. Malik and H. U. Amin, *Designing EEG Experiments for Studying the Brain: Design Code and Example Datasets*. Academic Press, 2017. Accessed: Aug. 04, 2023. [Online]. Available: <https://www.perlego.com/book/1828444/designing-eeg-experiments-for-studying-the-brain-design-code-and-example-datasets-pdf>

- [36] P. Abhang, B. Gawali, and S. Mehrotra, "Technical Aspects of Brain Rhythms and Speech Parameters," 2016, pp. 51–79. doi: 10.1016/B978-0-12-804490-2.00003-8.
- [37] P. Pandey, R. Tripathi, and K. Miyapuram, "Classifying oscillatory brain activity associated with Indian Rasas using network metrics," *Brain Inform.*, vol. 9, Dec. 2022, doi: 10.1186/s40708-022-00163-7.
- [38] "10–20 system (EEG)," *Wikipedia*. Mar. 16, 2023. Accessed: Aug. 04, 2023. [Online]. Available: [https://en.wikipedia.org/w/index.php?title=10%E2%80%9320_system_\(EEG\)&oldid=1144970353](https://en.wikipedia.org/w/index.php?title=10%E2%80%9320_system_(EEG)&oldid=1144970353)
- [39] M. Soufineyestani, D. Dowling, and A. Khan, "Electroencephalography (EEG) Technology Applications and Available Devices," *Appl. Sci.*, vol. 10, no. 21, Art. no. 21, Jan. 2020, doi: 10.3390/app10217453.
- [40] J. N. Acharya, A. Hani, J. Cheek, P. Thirumala, and T. N. Tsuchida, "American Clinical Neurophysiology Society Guideline 2: Guidelines for Standard Electrode Position Nomenclature," *J. Clin. Neurophysiol. Off. Publ. Am. Electroencephalogr. Soc.*, vol. 33, no. 4, pp. 308–311, Aug. 2016, doi: 10.1097/WNP.0000000000000316.
- [41] B. Products, "Getting to know EEG artifacts and how to handle them in BrainVision Analyzer," *Brain Products Press Release*, Dec. 09, 2022. <https://pressrelease.brainproducts.com/eeg-artifacts-handling-in-analyzer/> (accessed May 15, 2023).
- [42] "Artifacts in EEG Data — Data Science for Psychology and Neuroscience — in Python." https://neuraldatascience.io/7-eeg/erp_artifacts.html (accessed May 15, 2023).
- [43] X. Jiang, G.-B. Bian, and Z. Tian, "Removal of Artifacts from EEG Signals: A Review," *Sensors*, vol. 19, no. 5, p. 987, Feb. 2019, doi: 10.3390/s19050987.
- [44] D. S. Touretzky, M. C. Mozer, and M. E. Hasselmo, *Advances in Neural Information Processing Systems 8: Proceedings of the 1995 Conference*. MIT Press, 1996.
- [45] C. Schönbach, S. Ranganathan, K. Nakai, M. Gribskov, M. A. Khan, and M. Cannataro, *Encyclopedia of Bioinformatics and Computational Biology: Applications / Mohammad Asif Khan (Centre for Bioinformatics, Perdana University, Selangor, Malaysia)*. Elsevier, 2018.
- [46] C. K. M. PhD, Ed., *Encyclopedia of Sleep*, 1st edition. Amsterdam: Academic Press, 2013.
- [47] "Welcome — Data Science for Psychology and Neuroscience — in Python." <https://neuraldatascience.io/intro.html> (accessed Nov. 29, 2022).
- [48] J. M. Blackledge, Ed., "Digital Signal Processing," in *Digital Signal Processing (Second Edition)*, in Woodhead Publishing Series in Electronic and Optical Materials. Woodhead Publishing, 2006, p. i. doi: 10.1016/B978-1-904275-26-8.50019-1.
- [49] G. Ellis, *Control System Design Guide: Using Your Computer to Understand and Diagnose Feedback Controllers*, 4th edition. Butterworth-Heinemann, 2016.
- [50] I. Grout, *Digital Systems Design with FPGAs and CPLDs*. Elsevier, 2011.
- [51] N. Kehtarnavaz, *Digital Signal Processing System Design: LabVIEW-Based Hybrid Programming*, 2nd edition. Amsterdam ; Boston: Academic Press, 2008.
- [52] *Biomedical Signal Analysis for Connected Healthcare por Sridhar Krishnan - Ebook | Scribd*. Accessed: Aug. 05, 2023. [Online]. Available: <https://www.scribd.com/book/512959974/Biomedical-Signal-Analysis-for-Connected-Healthcare>
- [53] O. Faust, U. R. Acharya, H. Adeli, and A. Adeli, "Wavelet-based EEG processing for computer-aided seizure detection and epilepsy diagnosis," *Seizure*, vol. 26, pp. 56–64, Mar. 2015, doi: 10.1016/j.seizure.2015.01.012.
- [54] V. Pukhova, E. Gorelova, G. Ferrini, and S. Burnasheva, "Time-frequency representation of signals by wavelet transform," in *2017 IEEE Conference of Russian Young Researchers in Electrical and Electronic Engineering (EIConRus)*, Feb. 2017, pp. 715–718. doi: 10.1109/EIConRus.2017.7910658.


- [55] I. Stancin, M. Cifrek, and A. Jovic, "A Review of EEG Signal Features and their Application in Driver Drowsiness Detection Systems," *Sensors*, vol. 21, no. 11, p. 3786, May 2021, doi: 10.3390/s21113786.
- [56] M. P. Kalashami, M. M. Pedram, and H. Sadr, "EEG Feature Extraction and Data Augmentation in Emotion Recognition," *Comput. Intell. Neurosci.*, vol. 2022, p. e7028517, Mar. 2022, doi: 10.1155/2022/7028517.
- [57] "Calculations for Molecular Biology and Biotechnology - 3rd Edition." <https://shop.elsevier.com/books/calculations-for-molecular-biology-and-biotechnology/stephenson/978-0-12-802211-5> (accessed Jul. 14, 2023).
- [58] M. Jambu, *Exploratory and Multivariate Data Analysis*, 1st edition. Boston: Academic Press, 1991.
- [59] J. Slavič, Ed., *Vibration fatigue by spectral methods: from structural dynamics to fatigue damage -- theory and experiments*. Amsterdam: Elsevier, 2021.
- [60] L.-C. Shi, Y.-Y. Jiao, and B.-L. Lu, "Differential entropy feature for EEG-based vigilance estimation," in *2013 35th Annual International Conference of the IEEE Engineering in Medicine and Biology Society (EMBC)*, Jul. 2013, pp. 6627–6630. doi: 10.1109/EMBC.2013.6611075.
- [61] S. T. Grafton and L. J. Volz, "Chapter 13 - From ideas to action: The prefrontal–premotor connections that shape motor behavior," in *Handbook of Clinical Neurology*, M. D'Esposito and J. H. Grafman, Eds., in *The Frontal Lobes*, vol. 163. Elsevier, 2019, pp. 237–255. doi: 10.1016/B978-0-12-804281-6.00013-6.
- [62] B. Ellenbroek and J. Youn, "Chapter 9 - Schizophrenia," in *Gene-Environment Interactions in Psychiatry*, B. Ellenbroek and J. Youn, Eds., San Diego: Academic Press, 2016, pp. 289–322. doi: 10.1016/B978-0-12-801657-2.00009-4.
- [63] S. B. Eickhoff and V. I. Müller, "Functional Connectivity," in *Brain Mapping*, A. W. Toga, Ed., Waltham: Academic Press, 2015, pp. 187–201. doi: 10.1016/B978-0-12-397025-1.00212-8.
- [64] A. M. Bastos and J.-M. Schoffelen, "A Tutorial Review of Functional Connectivity Analysis Methods and Their Interpretational Pitfalls," *Front. Syst. Neurosci.*, vol. 9, 2016, Accessed: Jan. 18, 2023. [Online]. Available: <https://www.frontiersin.org/articles/10.3389/fnsys.2015.00175>
- [65] C. T. Briels, D. N. Schoonhoven, C. J. Stam, H. de Waal, P. Scheltens, and A. A. Gouw, "Reproducibility of EEG functional connectivity in Alzheimer's disease," *Alzheimers Res. Ther.*, vol. 12, no. 1, p. 68, Jun. 2020, doi: 10.1186/s13195-020-00632-3.
- [66] L. S. Imperatori *et al.*, "EEG functional connectivity metrics wPLI and wSMI account for distinct types of brain functional interactions," *Sci. Rep.*, vol. 9, no. 1, Art. no. 1, Jun. 2019, doi: 10.1038/s41598-019-45289-7.
- [67] I. Gaudet, A. Hüsner, P. Vannasing, and A. Gallagher, "Functional Brain Connectivity of Language Functions in Children Revealed by EEG and MEG: A Systematic Review," *Front. Hum. Neurosci.*, vol. 14, 2020, Accessed: Aug. 02, 2023. [Online]. Available: <https://www.frontiersin.org/articles/10.3389/fnhum.2020.00062>
- [68] W. R. Sherman and A. B. Craig, "Virtual Reality," in *Encyclopedia of Information Systems*, Elsevier, 2003, pp. 589–617. doi: 10.1016/B0-12-227240-4/00194-5.
- [69] S. Gillner and H. A. Mallot, "Virtual Reality and Spatial Cognition," in *International Encyclopedia of the Social & Behavioral Sciences*, N. J. Smelser and P. B. Baltes, Eds., Oxford: Pergamon, 2001, pp. 16211–16214. doi: 10.1016/B0-08-043076-7/00576-3.
- [70] "Lernen mit Virtual Reality," *Forbes*, Mar. 08, 2018. <https://www.forbes.at/artikel/lernen-mit-virtual-reality.html> (accessed Aug. 06, 2023).
- [71] G. Guazzaroni, *Virtual and Augmented Reality in Mental Health Treatment*. IGI Global, 1AD. Accessed: Aug. 06, 2023. [Online]. Available: <https://www.igi-global.com/book/virtual-augmented-reality-mental-health/www.igi-global.com/book/virtual-augmented-reality-mental-health/204118>
- [72] J. Diemer, P. Pauli, and A. Mühlberger, "Virtual Reality in Psychotherapy," in *International Encyclopedia of the Social & Behavioral Sciences (Second Edition)*, J. D. Wright, Ed., Oxford: Elsevier,

- 2015, pp. 138–146. doi: 10.1016/B978-0-08-097086-8.21070-2.
- [73] A. “Skip” Rizzo and R. Shilling, “Clinical Virtual Reality tools to advance the prevention, assessment, and treatment of PTSD,” *Eur. J. Psychotraumatology*, vol. 8, no. sup5, p. 1414560, 2017, doi: 10.1080/20008198.2017.1414560.
- [74] “SEED Dataset.” <https://bcmi.sjtu.edu.cn/~seed/seed-iv.html#> (accessed Aug. 29, 2023).
- [75] N. S. Suhaimi, J. Mountstephens, and J. Teo, “A Dataset for Emotion Recognition Using Virtual Reality and EEG (DER-VREEG): Emotional State Classification Using Low-Cost Wearable VR-EEG Headsets,” *Big Data Cogn. Comput.*, vol. 6, no. 1, Art. no. 1, Mar. 2022, doi: 10.3390/bdcc6010016.
- [76] “EEG Looming.” <https://www.kaggle.com/datasets/vicolab/eeg-looming> (accessed Aug. 29, 2023).
- [77] E. A. Phelps and J. E. LeDoux, “Contributions of the amygdala to emotion processing: from animal models to human behavior,” *Neuron*, vol. 48, no. 2, pp. 175–187, Oct. 2005, doi: 10.1016/j.neuron.2005.09.025.
- [78] B. J. Liddell *et al.*, “A direct brainstem-amygdala-cortical ‘alarm’ system for subliminal signals of fear,” *NeuroImage*, vol. 24, no. 1, pp. 235–243, Jan. 2005, doi: 10.1016/j.neuroimage.2004.08.016.
- [79] “Get Mixed Reality Portal from the Microsoft Store.” <https://apps.microsoft.com/store/detail/mixed-reality-portal/9NG1H8B3ZC7M?hl=pt-pt&gl=pt> (accessed Sep. 13, 2023).
- [80] “HP Reverb G2 The no-compromise VR headset - TEK-Shanghai.” <https://tekshanghai.com/product/hp-reverb-g2-the-no-compromise-vr-headset/> (accessed Aug. 29, 2023).
- [81] “QuickTime Video, Apple ProRes 422 Codec Family,” Dec. 11, 2020. <https://www.loc.gov/preservation/digital/formats/fdd/fdd000429.shtml> (accessed Sep. 13, 2023).
- [82] “The WebM Project | About WebM.” <https://www.webmproject.org/about/> (accessed Sep. 13, 2023).
- [83] “Micromed - SystemPLUS Evolution. Get the software safely and easily.” *Software Informer*, Nov. 03, 2022. <https://micromed-systemplus-evolution.software.informer.com/> (accessed Sep. 13, 2023).
- [84] “Electro-Cap EEG Cap International 10-20 System - NeuroEvolution® - EEG, SEEG, EMG, PSG, TCD & IONM.” <https://neuroevolution.pt/pt/product/electro-cap-eeg-cap-10-20-system/> (accessed Aug. 08, 2023).
- [85] R. A. Armstrong, “When to use the Bonferroni correction,” *Ophthalmic Physiol. Opt. J. Br. Coll. Ophthalmic Opt. Optom.*, vol. 34, no. 5, pp. 502–508, Sep. 2014, doi: 10.1111/opo.12131.
- [86] D. Gabbay, P. Thagard, J. Woods, P. Bandyopadhyay, and M. Forster, *Philosophy of Statistics*, vol. 7. 2011.
- [87] G. Nolte, O. Bai, L. Wheaton, Z. Mari, S. Vorbach, and M. Hallett, “Identifying true brain interaction from EEG data using the imaginary part of coherency,” *Clin. Neurophysiol. Off. J. Int. Fed. Clin. Neurophysiol.*, vol. 115, no. 10, pp. 2292–2307, Oct. 2004, doi: 10.1016/j.clinph.2004.04.029.
- [88] E. Ortiz, K. Stingl, J. Münßinger, C. Braun, H. Preissl, and P. Belardinelli, “Weighted Phase Lag Index and Graph Analysis: Preliminary Investigation of Functional Connectivity during Resting State in Children,” *Comput. Math. Methods Med.*, vol. 2012, p. 186353, 2012, doi: 10.1155/2012/186353.
- [89] F. Mormann, K. Lehnertz, P. David, and C. Elger, “Mean phase coherence as a measure for phase synchronization and its application to the EEG of epilepsy patients,” *Phys. Nonlinear Phenom.*, vol. 144, pp. 358–369, Oct. 2000, doi: 10.1016/S0167-2789(00)00087-7.
- [90] K. J. Blinowska, “Review of the methods of determination of directed connectivity from multichannel data,” *Med. Biol. Eng. Comput.*, vol. 49, no. 5, pp. 521–529, 2011, doi: 10.1007/s11517-011-0739-x.
- [91] C. L. Scrivener and A. T. Reader, “Variability of EEG electrode positions and their underlying brain

- regions: visualizing gel artifacts from a simultaneous EEG-fMRI dataset," *Brain Behav.*, vol. 12, no. 2, p. e2476, Feb. 2022, doi: 10.1002/brb3.2476.
- [92] "Brodmann Areas: Anatomy and Functions," Nov. 03, 2022. <https://www.simplypsychology.org/brodmann-areas.html> (accessed Aug. 08, 2023).
- [93] "Visual Processing: Cortical Pathways (Section 2, Chapter 15) Neuroscience Online: An Electronic Textbook for the Neurosciences | Department of Neurobiology and Anatomy - The University of Texas Medical School at Houston." <https://nba.uth.tmc.edu/neuroscience/m/s2/chapter15.html> (accessed Aug. 08, 2023).
- [94] K. Grill-Spector, Z. Kourtzi, and N. Kanwisher, "The lateral occipital complex and its role in object recognition," *Vision Res.*, vol. 41, no. 10–11, pp. 1409–1422, 2001, doi: 10.1016/s0042-6989(01)00073-6.
- [95] "Brodmann areas," *Kenhub*. <https://www.kenhub.com/en/library/anatomy/brodmann-areas> (accessed Aug. 08, 2023).
- [96] L. Banker and P. Tadi, "Neuroanatomy, Precentral Gyrus," in *StatPearls*, Treasure Island (FL): StatPearls Publishing, 2023. Accessed: Aug. 08, 2023. [Online]. Available: <http://www.ncbi.nlm.nih.gov/books/NBK544218/>
- [97] "Primary Somatosensory Cortex - an overview | ScienceDirect Topics." <https://www.sciencedirect.com/topics/medicine-and-dentistry/primary-somatosensory-cortex> (accessed Aug. 08, 2023).
- [98] E. Kropf, S. K. Syan, L. Minuzzi, and B. N. Frey, "From anatomy to function: the role of the somatosensory cortex in emotional regulation," *Rev. Bras. Psiquiatr.*, vol. 41, no. 3, pp. 261–269, Dec. 2018, doi: 10.1590/1516-4446-2018-0183.
- [99] B. R. Buchsbaum, G. Hickok, and C. Humphries, "Role of left posterior superior temporal gyrus in phonological processing for speech perception and production," *Cogn. Sci.*, vol. 25, no. 5, pp. 663–678, 2001, doi: 10.1207/s15516709cog2505_2.
- [100] J. T. Walkup, S. J. Friedland, T. S. Peris, and J. R. Strawn, "Dysregulation, Catastrophic Reactions, and the Anxiety Disorders," *Child Adolesc. Psychiatr. Clin. N. Am.*, vol. 30, no. 2, pp. 431–444, Apr. 2021, doi: 10.1016/j.chc.2020.10.011.
- [101] D. Cazzoli, B. C. Kaufmann, R. E. Paladini, R. M. Müri, T. Nef, and T. Nyffeler, "Anterior insula and inferior frontal gyrus: where ventral and dorsal visual attention systems meet," *Brain Commun.*, vol. 3, no. 1, p. fcaa220, Jan. 2021, doi: 10.1093/braincomms/fcaa220.
- [102] M. J. Herrmann, J. S. Beier, B. Simons, and T. Polak, "Transcranial Direct Current Stimulation (tDCS) of the Right Inferior Frontal Gyrus Attenuates Skin Conductance Responses to Unpredictable Threat Conditions," *Front. Hum. Neurosci.*, vol. 10, 2016, Accessed: Aug. 09, 2023. [Online]. Available: <https://www.frontiersin.org/articles/10.3389/fnhum.2016.00352>
- [103] A. L. Gold, R. A. Morey, and G. McCarthy, "Amygdala–Prefrontal Cortex Functional Connectivity During Threat-Induced Anxiety and Goal Distraction," *Biol. Psychiatry*, vol. 77, no. 4, pp. 394–403, Feb. 2015, doi: 10.1016/j.biopsych.2014.03.030.
- [104] L. Sagliano, M. Vela, L. Trojano, and M. Conson, "The role of the right premotor cortex and temporo-parietal junction in defensive responses to visual threats," *Cortex*, vol. 120, pp. 532–538, Nov. 2019, doi: 10.1016/j.cortex.2019.08.005.
- [105] H. Duffau, "Chapter 6 - Cortical and Subcortical Brain Mapping," in *Schmidek and Sweet Operative Neurosurgical Techniques (Sixth Edition)*, A. Quiñones-Hinojosa, Ed., Philadelphia: W.B. Saunders, 2012, pp. 80–93. doi: 10.1016/B978-1-4160-6839-6.10006-1.
- [106] P. Johns, "Chapter 13 - Parkinson's disease," in *Clinical Neuroscience*, P. Johns, Ed., Churchill Livingstone, 2014, pp. 163–179. doi: 10.1016/B978-0-443-10321-6.00013-8.
- [107] M. K. Madsen, B. Mc Mahon, S. B. Andersen, H. R. Siebner, G. M. Knudsen, and P. M. Fisher, "Threat-related amygdala functional connectivity is associated with 5-HTTLPR genotype and neuroticism," *Soc. Cogn. Affect. Neurosci.*, vol. 11, no. 1, pp. 140–149, Jan. 2016, doi: 10.1093/scan/nsv098.

- [108] P. A. Kirk, A. J. Holmes, and O. J. Robinson, “Threat vigilance and intrinsic amygdala connectivity,” *Hum. Brain Mapp.*, vol. 43, no. 10, pp. 3283–3292, Jul. 2022, doi: 10.1002/hbm.25851.
- [109] D. Purves *et al.*, “The Premotor Cortex,” in *Neuroscience. 2nd edition*, Sinauer Associates, 2001. Accessed: Sep. 05, 2023. [Online]. Available: <https://www.ncbi.nlm.nih.gov/books/NBK10796/>

Annex 1

	INFORMAÇÃO AO PARTICIPANTE E FORMULÁRIO DE CONSENTIMENTO INFORMADO	Referência	Versão CI
		Revisão	2.0
		Data	26-05-2022
Comissão de Ética	Página 1 de 108		

TÍTULO DO PROJETO DE INVESTIGAÇÃO:

Atividade cerebral registada por EEG durante a visualização de vídeos de realidade virtual

PROMOTOR:

FCTUC, Universidade de Coimbra

INVESTIGADOR COORDENADOR/ORIENTADOR:

Lorena Petrella

CENTRO DE ESTUDO CLÍNICO:

CISUC - Centro de Informática e Sistemas

INVESTIGADOR:

César Teixeira

MORADA:

Polo II, Pinhal de Marrocos, 3030-290, Coimbra

CONTACTO TELEFÓNICO:

239790090

NOME DO PARTICIPANTE:

É convidado(a) a participar voluntariamente neste estudo que envolve a visualização de um vídeo de realidade virtual enquanto são registados sinais de eletroencefalografia (EEG). O objetivo do estudo é analisar a evolução destes sinais ao longo da visualização do vídeo.

As informações que se seguem destinam-se a esclarecê-lo acerca da natureza, alcance, consequências e risco do estudo, de modo a permitir que, depois de esclarecido, se encontre capaz de decidir participar, ou não, neste estudo.

Caso não tenha qualquer dúvida acerca do mesmo, deverá tomar a decisão de participar ou não. Se não quiser participar não sofrerá qualquer tipo de penalização. Caso queira participar, ser-lhe-á solicitado que assine e date este formulário.

Após a sua assinatura e a do Investigador, ser-lhe-á entregue uma cópia, que deve guardar.

1. INFORMAÇÃO GERAL E OBJETIVOS DO ESTUDO

Este estudo irá decorrer no Centro de Informática e Sistemas da Universidade de Coimbra (CISUC) e tem por objetivo a análise da evolução dos sinais de eletroencefalografia (EEG) adquiridos ao longo da visualização do vídeo de realidade virtual. Trata-se de um estudo clínico sem intervenção.

Este estudo foi aprovado pela Comissão de Ética da Faculdade de Medicina da Universidade de Coimbra

(FMUC), de modo a garantir a proteção dos direitos, segurança e bem-estar de todos os participantes incluídos e garantir prova pública dessa proteção.

2. PLANO E METODOLOGIA DO ESTUDO

Para participar neste estudo deve ter entre 18 e 40 anos. Não pode participar se apresenta alguma das seguintes características: défices visuais, condições neuropatológicas, uso de psicofármacos ou patologias cardíacas. Durante a sessão, deverá estar confortavelmente sentado e uma pessoa treinada irá acoplar, mediante o uso de gel, diversos elétrodos (pequenos) em diferentes posições do couro cabeludo. Este acoplamento é externo e não causa dor nem riscos. Uma vez acoplados os eletrodos, ser-lhe-ão colocados óculos de realidade virtual e um vídeo é reproduzido. Durante este período, deverá manter-se calmo e observar o vídeo. Após a visualização do vídeo, os equipamentos serão retirados e ser-lhe-ão fornecidas toalhas (ou afins) para limpar o excedente de gel utilizado para acoplar os eletrodos. Todo o procedimento durará aproximadamente uma hora e a participação do voluntário limita-se a uma única sessão. A data prevista de início do estudo é 02/01/2023 e a de conclusão é 14/07/2023.

3. PROTEÇÃO DE DADOS DOS PARTICIPANTES

3.1 Responsável pelos dados

Lorena Petrella

3.2 Recolha de dados

Recolha direta (ao próprio) presencial

3.3 Categorias de dados

Idade e dados relativos à saúde

3.4 Tratamento de dados

Os dados recolhidos serão guardados em formato digital protegido.

3.5 Medidas de proteção adotadas

O participante é identificado por código de 3 dígitos especificamente criado para este estudo, sendo o investigador quem realiza a codificação dos dados.

3.6 Prazo de conservação dos dados

10 anos

3.7 Informação em caso de publicação

A confidencialidade da identidade e dos dados do voluntário é assegurada.

4. RISCOS E POTENCIAIS INCONVENIENTES PARA O PARTICIPANTE

A realização do estudo não implica qualquer risco, efeito adverso e/ou inconveniente para o participante.

O único incómodo previsível é a colocação de gel no couro cabeludo utilizado no acoplamento dos eletrodos para registro de EEG.

Não são esperados incômodos relacionados ao vídeo de realidade virtual, nem devidos ao questionário.

Estima-se que a duração do procedimento completo seja inferior a 1h.

5. POTENCIAIS BENEFÍCIOS

A participação no estudo não traz benefícios imediatos para os participantes.

6. NOVAS INFORMAÇÕES

Não se aplica

7. RESPONSABILIDADE CIVIL

Não se aplica

8. PARTICIPAÇÃO / RETIRADA DO CONSENTIMENTO

É inteiramente livre de aceitar ou recusar participar neste estudo. Pode retirar o seu consentimento em qualquer altura, através da notificação ao investigador, sem qualquer consequência, sem precisar de explicar as razões, sem qualquer penalização ou perda de benefícios e sem comprometer a sua relação com o investigador que lhe propõe a participação neste estudo.

O consentimento entretanto retirado não abrange os dados recolhidos e tratados até a essa data.

O investigador do estudo pode decidir terminar a sua participação neste estudo se entender que não é do melhor interesse continuar nele. A sua participação pode também terminar se o plano do estudo não estiver a ser cumprido. O investigador notificará-lo-á se surgir uma dessas circunstâncias.

9. CONFIDENCIALIDADE

Será garantido o respeito pelo direito do participante à sua privacidade e à proteção dos seus dados pessoais; devendo ainda ser assegurado que será cumprido o dever de sigilo e de confidencialidade a que se encontra vinculado, conforme disposto no artigo 29.º da Lei n.º 58/2019, de 08/08.

10 – DIREITO DE ACESSO E RETIFICAÇÃO

Pode exercer o direito de acesso, retificação e oposição ao tratamento dos seus dados. Contudo, este direito pode ser sujeito a limitações, de acordo com a Lei.

11. REEMBOLSO E/OU RESSARCIMENTO DO PARTICIPANTE

Este estudo é da iniciativa do investigador e, por isso, solicita-se a sua participação sem uma compensação financeira para a sua colaboração.

12. COMPENSAÇÃO DO CENTRO DE ESTUDO / INVESTIGADOR

O investigador não receberá compensação financeira pelo seu trabalho na realização do estudo.

13. CONTACTOS

Se tiver questões sobre este estudo deve contactar:

Investigador	Lorena Petrella
Morada	Polo II, Pinhal de Marrocos, 3030-290, Coimbra
Telefone	Não se aplica
Email	lorenapetrella@dei.uc.pt

Se tiver dúvidas relativas aos seus direitos como participante deste estudo, poderá contactar:

Presidente da Comissão de Ética da FMUC
Universidade de Coimbra • Faculdade de Medicina
Pólo das Ciências da Saúde • Unidade Central Azinhaga de Santa Comba, Celas
3000-354 COIMBRA • PORTUGAL
Tel.: +351 239 857 708 (Ext. 542708) | Fax: +351 239 823 236
E-mail: comissaoetica@fmed.uc.pt | www.fmed.uc.pt

NÃO ASSINE O FORMULÁRIO DE CONSENTIMENTO INFORMADO A MENOS QUE TENHA TIDO A OPORTUNIDADE DE PERGUNTAR E TER RECEBIDO RESPOSTAS SATISFATÓRIAS A TODAS AS SUAS PERGUNTAS.

CONSENTIMENTO INFORMADO

Título do Projeto de Investigação

Nome do Participante:	
BI / CC:	Contactos:
Nome do Investigador:	

No âmbito da realização do Projeto de Investigação acima mencionado, declaro que tomei conhecimento:

- do conteúdo informativo anexo a este formulário e aceito, de forma voluntária, participar neste estudo;
- da natureza, alcance, consequências, potenciais riscos e duração prevista do estudo, assim como do que é esperado da minha parte, enquanto participante;
- e compreendi as informações e esclarecimentos que me foram dados. Sei que a qualquer momento poderei colocar novas questões ao investigador responsável pelo estudo;
- que o investigador se compromete a prestar qualquer informação relevante que surja durante o estudo e que possa alterar a minha vontade de continuar a participar;
- e aceito cumprir o protocolo deste estudo. Comprometo-me ainda a informar o investigador de eventuais alterações do meu estado de saúde que possam ocorrer (*quando*

aplicável);

- f. e autorizo a utilização e divulgação dos resultados do estudo para fins exclusivamente científicos e permito a divulgação desses resultados às autoridades competentes;
- g. que posso exercer o meu direito de retificação e/ou oposição, nos limites da Lei;
- h. que sou livre de desistir do estudo a qualquer momento, sem ter de justificar a minha decisão e sem sofrer qualquer penalização. Sei também que os dados recolhidos e tratados até a essa data serão mantidos;
- i. que o investigador tem o direito de decidir sobre a minha eventual saída prematura do estudo e se compromete a informar-me do respetivo motivo;
- j. que o estudo pode ser interrompido por decisão do investigador, do promotor ou das autoridades reguladoras.

Local e data:	Assinaturas
	Participante:
	Representante legal:
	Representante legal:
	Investigador (*):

(*) confirmo que expliquei ao participante acima mencionado a natureza, o alcance e os potenciais riscos do estudo acima mencionado.

Annex 2

Table A2.1: Participants information.

Code	Date	Age	Was the threat stimulus observed?	Did you felt threatened?
1	02/05 15h	23	Yes	Yes
2	03/05 11h	22	Yes	Yes
3	04/05 14h	18	Yes	Yes
4	04/05 18h	22	Yes	Yes
5	05/05 10h	22	Yes	Yes
6	05/05 11h	22	Yes	Yes
7	05/05 14h	32	Yes	No
8	08/05 16h	22	Yes	Yes
9	08/05 17h	18	Yes	No

10	09/05 13h30	29	Yes	Yes
11	10/05 10h	22	Yes	No
12	10/05 11h30	29	Yes	Yes
13	10/05 17h	22	Yes	Yes
14	10/05 18h	23	Yes	Yes
15	11/05 14h	19	Yes	Yes
16	16/05 10h30	30	Yes	Yes
17	16/05 11h30	35	Yes	No
18	16/05 13h	36	Yes	Yes
19	17/05 10h	24	Yes	Yes
20	26/06 14h30	22	Yes	Yes
21	03/07 9h30	29	Yes	Yes
22	03/07 11h30	26	Yes	No
23	18/07 18h30	22	Yes	Yes
24	19/07 16h30	22	Yes	Yes
25	20/07 14h30	25	Yes	No
26	21/07 10h	22	Yes	Yes